

# Cross Sections and Swarm Coefficients for $H^+$ , $H_2^+$ , $H_3^+$ , H, $H_2$ , and $H^-$ in $H_2$ for Energies from 0.1 eV to 10 keV

Cite as: Journal of Physical and Chemical Reference Data **19**, 653 (1990); <https://doi.org/10.1063/1.555858>  
Submitted: 05 July 1989 . Published Online: 15 October 2009

A. V. Phelps



View Online



Export Citation

## ARTICLES YOU MAY BE INTERESTED IN

### Cross Sections and Related Data for Electron Collisions with Hydrogen Molecules and Molecular Ions

Journal of Physical and Chemical Reference Data **19**, 617 (1990); <https://doi.org/10.1063/1.555856>

### Cross Sections for Electron Collisions with Hydrogen Molecules

Journal of Physical and Chemical Reference Data **37**, 913 (2008); <https://doi.org/10.1063/1.2838023>

Erratum: Cross Sections and Swarm Coefficients for  $H^+$ ,  $H_2^+$ ,  $H_3^+$ , H,  $H_2$ , and  $H^-$  in  $H_2$  for Energies from 0.1 eV to 10 keV [J. Phys. Chem. Ref. Data **19**, 653 (1990)]

Journal of Physical and Chemical Reference Data **20**, 1339 (1991); <https://doi.org/10.1063/1.555904>

Where in the **world** is AIP Publishing?  
*Find out where we are exhibiting next*



# Cross Sections and Swarm Coefficients for $H^+$ , $H_2^+$ , $H_3^+$ , $H$ , $H_2$ , and $H^-$ in $H_2$ for Energies from 0.1 eV to 10 keV

A. V. Phelps

Joint Institute for Laboratory Astrophysics, University of Colorado and National Institute of Standards and Technology, Boulder, Colorado 80309-0440

Received July 5, 1989; revised manuscript received January 12, 1990

Graphical and tabulated data and the associated bibliography are presented for cross sections for elastic, excitation and ionization collisions of  $H^+$ ,  $H_2^+$ ,  $H_3^+$ ,  $H$ ,  $H_2$ , and  $H^-$  with  $H_2$  at laboratory energies from 0.1 to 10 keV. Where appropriate, drift velocities and reaction or excitation coefficients are calculated from the cross sections and recommended for use in analyses of swarm experiments and electrical discharges. In the case of  $H^+$  in  $H_2$ , cross sections for momentum transfer, rotational excitation, vibrational excitation, charge transfer, electronic excitation, and ionization are recommended. Energy-loss or stopping-power coefficients calculated from these cross sections are much smaller than obtained from stopping-power theory. There are no relevant energy-loss experiments for  $H^+$  in  $H_2$ . Drift velocity calculations predict runaway for  $H^+$  in  $H_2$  for electric field to gas density ratios  $E/n$  greater than 700 Td, where 1 Td (townsend) =  $10^{-21}$  V m<sup>2</sup>. For  $H_2^+$  in  $H_2$ , the cross sections include  $H_3^+$  formation, charge transfer, vibrational and electronic excitation, and ionization. Drift velocities and average cross sections are calculated for  $E/n > 1$  kTd. For  $H_3^+$  in  $H_2$ , cross sections for momentum transfer, various charge transfer processes, electronic excitation, and ionization and drift velocities are recommended. In the case of  $H$  in  $H_2$ , cross sections for momentum transfer, rotational excitation, vibrational excitation, charge transfer,  $H^-$  formation, electronic excitation, and ionization are recommended. For  $H_2$  in  $H_2$ , cross sections for momentum transfer, rotational excitation, vibrational excitation, charge transfer, electronic excitation, and ionization are recommended. In the case of  $H^-$  in  $H_2$ , cross sections for momentum transfer, electron detachment, and ionization are recommended and calculated drift velocities are compared with experiment. Collisions of electronically excited states with  $H_2$  are not included.

**Key words:** charge transfer; cross section; data compilation; dissociation; electronic excitation; fast neutrals; hydrogen; ionization; ions; momentum transfer; rotational excitation; swarm coefficient; vibrational excitation.

## Contents

|  |     |   |     |
|--|-----|---|-----|
| 1. Introduction .....  | 654 | 5.1. $H_3^+$ - $H_2$ Cross Sections .....                     | 664 |
| 2. Symbols .....   | 655 | 5.2. Drift Velocity and Destruction of $H_3^+$ in $H_2$ ..... | 665 |
| 3. $H^+$ Collisions with $H_2$ .....                                       | 655 | 6. $H$ Collisions with $H_2$ .....                            | 666 |
| 3.1. $H^+$ - $H_2$ Cross Sections .....                                    | 655 | 6.1. $H$ - $H_2$ Cross Sections .....                         | 666 |
| 3.2. Energy, Momentum Loss, and Stopping Power for $H^+$ in $H_2$ .....    | 657 | 6.2. Stopping Power for $H$ in $H_2$ .....                    | 667 |
| 3.3. Drift Velocities and Reaction Coefficients for $H^+$ in $H_2$ .....   | 660 | 7. $H_2$ Collisions with $H_2$ .....                          | 670 |
| 4. $H_2^+$ Collisions with $H_2$ .....                                     | 661 | 7.1. $H_2$ - $H_2$ Cross Sections .....                       | 670 |
| 4.1. $H_2^+$ - $H_2$ Cross Sections .....                                  | 661 | 7.2. $H_2$ - $H_2$ Average Cross Sections .....               | 670 |
| 4.2. Drift Velocities and Reaction Coefficients for $H_2^+$ in $H_2$ ..... | 663 | 8. $H^-$ Collisions with $H_2$ .....                          | 670 |
| 5. $H_3^+$ Collisions with $H_2$ .....                                     | 664 | 9. Discussion .....   | 672 |
|  |     | 10. Acknowledgments .....                                     | 673 |
|  |     | 11. References .....  | 674 |

©1990 by the U. S. Secretary of Commerce on behalf of the United States. This copyright is assigned to the American Institute of Physics and the American Chemical Society.  
Reprints available from ACS; see Reprints List at back of issue.

## List of Tables

|   |     |
|---|-----|
| 1. Cross sections for $H^+$ + $H_2$ collisions by product. .... | 656 |
|---|-----|

|   |     |  |     |
|---|-----|--|-----|
| 2. Energy and momentum loss functions for $H^+ + H_2$ tabulated by product. ....            | 659 | 2. Energy loss $L_\epsilon$ and momentum loss $L_m$ coefficients for $H^+$ in $H_2$ versus $H^+$ laboratory energy. ....                         | 658 |
| 3. Calculated steady-state energies and drift velocities for $H^+$ in $H_2$ . ....          | 660 | 3. Drift velocities $W_\epsilon$ and $W_m$ and effective destruction cross section $Q_d$ for $H^+$ in $H_2$ versus $E/n$ . ....                  | 660 |
| 4. Cross sections for $H_2^+ + H_2$ collisions by product. ....                             | 662 | 4. Cross sections for collisions of $H_2^+$ with $H_2$ versus laboratory energy of $H_2^+$ for $H_2$ at rest. ....                               | 661 |
| 5. Calculated transport coefficients and average cross sections for $H_2^+$ in $H_2$ . .... | 664 | 5. Average cross sections, drift velocities $W^+$ , and ion "temperature" $T_+$ as a function of $E/n$ for $H_2^+$ drifting through $H_2$ . .... | 663 |
| 6. Cross sections for $H_3^+ + H_2$ collisions tabulated by product. ....                   | 665 | 6. Cross sections for collisions of $H_3^+$ with $H_2$ versus laboratory energy of $H_3^+$ for $H_2$ at rest. ....                               | 664 |
| 7. Drift velocities and destruction coefficients for $H_3^+$ and $H^-$ in $H_2$ . ....      | 666 | 7. Drift velocities $W(H_3^+)$ and $W(H^-)$ and destruction cross sections $Q_d(H_3^+)$ and $Q_d(H^-)$ in $H_2$ versus $E/n$ . ....              | 666 |
| 8. Cross sections for $H + H_2$ collisions tabulated by product. ....                       | 668 | 8. Cross sections for collisions of $H$ with $H_2$ versus laboratory energy of $H$ for $H_2$ at rest. ....                                       | 667 |
| 9. Energy loss functions for $H + H_2$ tabulated by product. ....                           | 669 | 9. Energy loss $L_\epsilon$ coefficients for $H$ in $H_2$ versus $H$ laboratory energy. ....   | 669 |
| 10. Cross sections for $H_2 + H_2$ collisions tabulated by product. ....                    | 671 | 10. Cross sections for collisions of $H_2$ with $H_2$ versus laboratory energy of the projectile $H_2$ for the target $H_2$ at rest. ....        | 670 |
| 11. Average cross sections for $H_2 + H_2$ collisions. ....                                 | 672 | 11. Average cross sections as a function of $E/n$ for $H_2$ formed from $H_2^+$ drifting through $H_2$ . ....                                    | 672 |
| 12. Cross sections for $H^- + H_2$ collisions tabulated by product. ....                    | 673 | 12. Cross sections for collisions of $H^-$ with $H_2$ versus laboratory energy of $H^-$ for $H_2$ at rest. ....                                  | 672 |

### List of Figures

|  |     |
|--|-----|
| 1. Cross sections for collisions of $H^+$ with $H_2$ versus laboratory energy of $H^+$ for $H_2$ at rest. .... | 655 |
|--|-----|

## 1. Introduction

This paper presents graphical and tabulated data and the associated bibliography for cross sections for elastic, excitation, and ionization collisions of  $H^+$ ,  $H_2^+$ ,  $H_3^+$ ,  $H$ ,  $H_2$ , and  $H^-$  in  $H_2$  for laboratory energies from 0.1 eV to 10 keV. Ion-transport and reaction coefficients calculated from these cross sections are compared with available experimental data and are tabulated.

The cross-section data were assembled from published results. The choices of data were guided by their intended use in the modeling of electrical discharges in weakly ionized  $H_2$ . The data are expected to find use in models of breakdown in  $H_2$  at low pressures,<sup>1</sup> the cathode fall of  $H_2$  discharges<sup>2-4</sup> at voltages above  $\sim 500$  V, hydrogen thyratrons,<sup>5</sup> ion sources,<sup>6,7</sup> and in "pseudospark" devices.<sup>8</sup> Studies utilizing similar data to analyze emission and breakdown measurements for discharges in  $N_2$  and Ar have been published.<sup>9-11</sup> Also, a number of reviews which include recommended cross sections for  $H^+$ ,  $H$ , and  $H_2^+$  collisions with  $H_2$  have appeared, or will appear soon; Green and McNeal,<sup>12</sup> Fedorenko,<sup>13</sup> Olson,<sup>14</sup> Barnett *et al.*,<sup>15</sup> Tawara,<sup>16</sup> Janev *et al.*,<sup>17</sup> Tawara *et al.*,<sup>18</sup> and Barnett *et al.*<sup>19</sup> We have made extensive use of these publications, both for citation and for background. Some of the lower energy processes considered in the present paper are discussed in connection with interstellar media models.<sup>20,21</sup> This review supersedes our conference report<sup>22</sup> and the summary of our  $H^+$  in  $H_2$

results by Inokuti and Berger.<sup>23</sup>

This paper is an effort to provide data of current need and is subject to revision as new data become available. The published cross sections have been interpolated and extrapolated where necessary to provide the "complete" sets of data needed for the models. We have not attempted to assign estimates of accuracy to the recommended data, but we have indicated areas of uncertainty and where extrapolations and interpolations were made. We have not considered gas mixtures or three-body collision processes. Collisions of electronically excited states of  $H$  and  $H_2$  with  $H_2$  are not included.

The cross sections and the transport and reaction coefficients for hydrogen ions and neutrals in  $H_2$  are shown in Figs. 1-12 and are listed in Tables 1-12. In general, the curves and tables are labeled by the experimentally observed or theoretically calculated product of the collision. Specific comments on the data are given in Secs. 3-8.

Unless otherwise specified, all energies are laboratory energies  $\epsilon_L$  rather than relative, center-of-mass, or "collision" energies. The same-logarithmic energy scale is used in all of the cross section and energy-loss tables because of the wide range of energies considered and the resultant simplicity of averages over the ion and fast neutral energy distributions. Although some entries in the tables are given to several significant figures, all entries should be considered uncertain to at least  $\pm 5\%$ . Blank entries in the tables indicate cross sections too small to be evaluated or zero.

## 2. Symbols

The symbols used in this paper are:

|                              |  |
|------------------------------|--|
| $d$                          | —electrode separation in m.  |
| $e$                          | —electronic charge = $1.602 \times 10^{-19}$ C.                                |
| $E/n$                        | —electric field to gas density ratio in Td.                                    |
| $J$                          | —quantum number of rotational level of $H_2$ or $H_2^+$ .                      |
| $L_e(x)$                     | —loss function for process $x$ in projectile energy balance in eV $m^2$ .      |
| $L_m(x)$                     | —loss function for process $x$ in projectile momentum balance in eV $m^2$ .    |
| $m$                          | —mass of projectile in kg.   |
| $M$                          | —mass of $H_2$ target in kg.   |
| $n$                          | —gas density in molecules/ $m^3$ .   |
| $n^*$                        | —principal quantum number of H atom or $H_2$ molecule.                         |
| $Q_{CT}$                     | —cross section for charge transfer collisions in $m^2$ .                       |
| $Q_o^i$                      | —total cross section for ionization in $m^2$ .                                 |
| $Q_o^k$                      | —total cross section for excitation for the $k^{\text{th}}$ process in $m^2$ . |
| $Q_d$                        | —cross section for “destruction” or loss of ions or fast neutrals in $m^2$ .   |
| $Q_m$                        | —momentum transfer cross section in $m^2$ .                                    |
| $\langle Q^k \rangle$        | —average cross section for process $k$ in $m^2$ .                              |
| $T_+$                        | —“temperature” characterizing energy distribution of $H_2^+$ ions in eV.       |
| Td                           | —unit of $E/n$ such that 1 Td (townsend) = $10^{-21}$ V $m^2$ .                |
| $v$                          | —quantum number of vibrational level of $H_2$ or $H_2^+$ molecule.             |
| $W^+$                        | —drift velocity of $H_2^+$ ions in m/s.  |
| $W(X^+)$                     | —drift velocity of $X^+$ ions in m/s.  |
| $W_e$                        | —drift velocity of $H^+$ calculated using energy balance model in m/s.         |
| $W_m$                        | —drift velocity of $H^+$ calculated using momentum balance model in m/s.       |
| $\alpha^k$                   | —spatial reaction or excitation coefficient for process $k$ in $m^{-1}$ .      |
| $\Delta J$                   | —change in rotational quantum number of $H_2$ or $H_2^+$ .                     |
| $\epsilon_L$                 | —projectile energy in the laboratory frame in eV.                              |
| $\langle \epsilon \rangle_i$ | —mean energy loss by projectile per ionizing collision in eV.                  |
| $\epsilon_k$                 | —energy loss in excitation of the $k^{\text{th}}$ level in eV.                 |
| $\epsilon_e$                 | —ion drift energy calculated using energy balance model in eV.                 |
| $\epsilon_m$                 | —ion drift energy calculated using momentum balance model in eV.               |
| $\Theta$                     | —angle of ion velocity vector with the electric field.                         |
| $\mu n$                      | —ion mobility normalized to unit density in $(m V s)^{-1}$ .                   |

## 3. $H^+$ Collisions with $H_2$

### 3.1. $H^+ - H_2$ Cross Sections

The momentum transfer cross section  $Q_m$  shown in Fig. 1 for  $\epsilon_L < 3.4$  eV was calculated from ion mobility data.<sup>24</sup> See Sec. 3.3. In our preliminary compilation of  $H^+ + H_2$  cross

sections, as summarized in Inokuti and Berger,<sup>23</sup> the differential-scattering cross-section calculations of Giese and Gentry<sup>25</sup> were used for  $9 < \epsilon_L < 38$  eV and were extrapolated to higher energies. Very recently, Stebbings<sup>26</sup> has made available to us tables of the  $H^+ + H_2$  differential-scattering data of Smith *et al.*<sup>27</sup> for energies of 500, 1500, and 5000 eV. Momentum-transfer cross sections for these energies are calculated by smoothly extrapolating the experimental differential-scattering data to the differential cross sections calculated using Coulomb scattering theory, as suggested by Newman *et al.*,<sup>28</sup> and integrating over scattering angle. The resultant momentum-transfer cross sections for  $\epsilon_L > 800$  eV are too small to show in Fig. 1, but are listed in Table 1. As shown by the short-dashed curve, we then interpolate between the results for  $\epsilon_L > 500$  eV and the values at low  $\epsilon_L$  derived from ion mobility. The resultant cross sections are about an order of magnitude larger than those calculated from the differential cross sections of Giese and Gentry<sup>25</sup> at 38 eV. Because of this large discrepancy, more theory and experiment for  $1 \text{ eV} < \epsilon_L < 1 \text{ keV}$  are important. Because of the dominance of Coulomb effects at large angles and  $\epsilon_L > 500$  eV, the  $Q_m$  values calculated from the  $H^+ - H_2$  differential-scattering data of Smith *et al.*<sup>27</sup> are close to those for H scattering by  $H_2$ , calculated from the data of Newman *et al.*<sup>28</sup> discussed in Sec. 6.1. Also, note that the total-scattering cross sections for  $H^+ + H_2$  collisions of Cramer<sup>29</sup> and of Linder<sup>30</sup> are much larger than the momentum-transfer cross sections, as expected for scattering, which is highly peaked in the forward direction.

The rotational-excitation cross sections shown in Fig. 1 are based on the very limited experimental data given by Linder<sup>30</sup> for  $6.8 < \epsilon_L < 15$  eV. For  $\epsilon_L < 0.6$  eV we have used

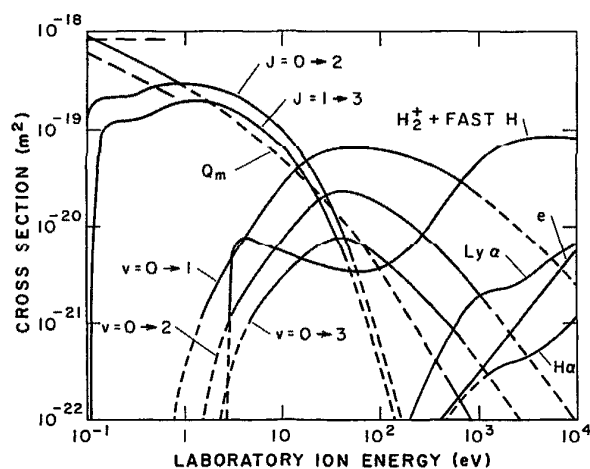


FIG. 1. Cross sections for collisions of  $H^+$  with  $H_2$  versus laboratory energy of  $H^+$  for  $H_2$  at rest. The solid curves are based on experiment or theory while the short-dashed curves are extrapolations or interpolations. The curves show cross sections for momentum transfer  $Q_m$ ; rotational excitation for  $J = 0 \rightarrow 2$  and  $J = 1 \rightarrow 3$ ; vibrational excitation for  $v = 0 \rightarrow 1$ ,  $0 \rightarrow 2$ , and  $0 \rightarrow 3$ ; charge transfer to  $H_2^+$  and fast H; Ly- $\alpha$  and H $\alpha$  excitation; and electron production ( $e$ ). The long-dashed lines are extrapolations to higher energies of fits of constant cross section and constant collision frequency models to 300 K mobility data. These cross sections are listed in Table 1.

Table 1. Cross sections for  $H^+ + H_2$  collisions tabulated by product(s).(Cross sections in units of  $10^{-20} \text{ m}^2$ )

| Lab. ion<br>energy<br>eV | Product |        |       |        |       |                             |         |         |         |                |
|--------------------------|---------|--------|-------|--------|-------|-----------------------------|---------|---------|---------|----------------|
|                          | J=0→2   | J=1→3  | V=0→1 | V=0→2  | V=0→3 | H <sub>2</sub> <sup>+</sup> | Ly α    | Hα      | Ioniz.  | Q <sub>m</sub> |
| 0.1                      | 13      |        |       |        |       |                             |         |         |         | 90             |
| 0.1334                   | 20      | 5      |       |        |       |                             |         |         |         | 79             |
| 0.1778                   | 21      | 11.7   |       |        |       |                             |         |         |         | 68             |
| 0.237                    | 21.4    | 12.3   |       |        |       |                             |         |         |         | 58             |
| 0.316                    | 22.5    | 12.8   |       |        |       |                             |         |         |         | 50.5           |
| 0.422                    | 26.5    | 14.2   |       |        |       |                             |         |         |         | 43.5           |
| 0.562                    | 28      | 16.4   |       |        |       |                             |         |         |         | 37.5           |
| 0.750                    | 29      | 18.5   |       |        |       |                             |         |         |         | 31.8           |
| 1.0                      | 29      | 19.8   | 0.039 |        |       |                             |         |         |         | 26.0           |
| 1.334                    | 28.7    | 20     | 0.088 |        |       |                             |         |         |         | 23.2           |
| 1.778                    | 27.3    | 19     | 0.173 | 0.023  |       |                             |         |         |         | 18.9           |
| 2.37                     | 25.2    | 17.8   | 0.296 | 0.066  | 0.012 |                             |         |         |         | 15.4           |
| 3.16                     | 22.5    | 15.7   | 0.51  | 0.133  | 0.043 | 0.59                        |         |         |         | 12.8           |
| 4.22                     | 19.8    | 13.3   | 0.79  | 0.213  | 0.09  | 0.75                        |         |         |         | 10.1           |
| 5.62                     | 16.4    | 10.9   | 1.22  | 0.325  | 0.143 | 0.71                        |         |         |         | 8.0            |
| 7.50                     | 13.2    | 8.6    | 1.78  | 0.5    | 0.21  | 0.615                       |         |         |         | 6.3            |
| 10.0                     | 9.8     | 6.6    | 2.65  | 0.72   | 0.29  | 0.54                        |         |         |         | 4.9            |
| 13.34                    | 7.2     | 4.8    | 3.6   | 1.03   | 0.395 | 0.48                        |         |         |         | 3.8            |
| 17.78                    | 4.8     | 3.1    | 4.6   | 1.45   | 0.51  | 0.435                       |         |         |         | 2.9            |
| 23.7                     | 2.85    | 1.93   | 5.45  | 1.86   | 0.63  | 0.397                       |         |         |         | 2.18           |
| 31.6                     | 1.6     | 1.08   | 6     | 2.2    | 0.73  | 0.365                       |         |         |         | 1.6            |
| 42.2                     | 0.8     | 0.55   | 6.3   | 2.3    | 0.75  | 0.34                        |         |         |         | 1.15           |
| 56.2                     | 0.36    | 0.245  | 6.35  | 2.2    | 0.7   | 0.333                       |         |         |         | 0.83           |
| 75.0                     | 0.15    | 0.095  | 6.3   | 1.98   | 0.59  | 0.34                        | 0.00077 |         | 0.00102 | 0.56           |
| 100.                     | 0.058   | 0.034  | 6.1   | 1.73   | 0.47  | 0.37                        | 0.00125 | 0.00097 | 0.0017  | 0.38           |
| 133.4                    | 0.021   | 0.012  | 5.75  | 1.45   | 0.38  | 0.43                        | 0.003   | 0.0016  | 0.0025  | 0.24           |
| 177.8                    | 0.0085  | 0.0046 | 5.4   | 1.2    | 0.29  | 0.54                        | 0.0074  | 0.0026  | 0.0037  | 0.14           |
| 237.                     | 0.0031  | 0.0017 | 4.9   | 0.93   | 0.22  | 0.73                        | 0.0155  | 0.0041  | 0.0054  | 0.082          |
| 316.                     | 0.0011  |        | 4.3   | 0.71   | 0.163 | 1.03                        | 0.029   | 0.006   | 0.0077  | 0.051          |
| 421.                     |         |        | 3.7   | 0.53   | 0.118 | 1.54                        | 0.053   | 0.0082  | 0.0109  | 0.032          |
| 562.                     |         |        | 3.15  | 0.39   | 0.083 | 2.3                         | 0.089   | 0.0137  | 0.0162  | 0.0195         |
| 750.                     |         |        | 2.6   | 0.275  | 0.058 | 3.35                        | 0.137   | 0.0198  | 0.023   | 0.0117         |
| 1000.                    |         |        | 2.15  | 0.198  | 0.04  | 4.5                         | 0.18    | 0.026   | 0.033   | 0.0072         |
| 1334.                    |         |        | 1.72  | 0.142  | 0.027 | 5.7                         | 0.207   | 0.0323  | 0.048   | 0.0045         |
| 1778.                    |         |        | 1.36  | 0.098  | 0.018 | 6.8                         | 0.224   | 0.038   | 0.069   | 0.0027         |
| 2371.                    |         |        | 1.06  | 0.068  | 0.012 | 7.6                         | 0.243   | 0.0415  | 0.088   | 0.00165        |
| 3162.                    |         |        | 0.81  | 0.047  | 0.008 | 8.2                         | 0.285   | 0.047   | 0.14    | 0.001          |
| 4217.                    |         |        | 0.61  | 0.0323 |       | 8.4                         | 0.365   | 0.055   | 0.2     | 0.00062        |
| 5623.                    |         |        | 0.455 | 0.0217 |       | 8.4                         | 0.45    | 0.068   | 0.28    | 0.00038        |
| 7499.                    |         |        | 0.325 | 0.0144 |       | 8.3                         | 0.54    | 0.088   | 0.4     | 0.000235       |
| 10000.                   |         |        | 0.235 | 0.0095 |       | 8.1                         | 0.65    | 0.12    | 0.55    | 0.000145       |

the near threshold behavior calculated by Gianturco and Tritella<sup>31</sup> for  $J = 0$  to  $J = 2$  excitation. These cross sections are somewhat smaller than those recommended by Janev *et al.*<sup>17</sup> In order to use these cross sections the values listed must be multiplied by the fraction of the  $H_2$  molecules in the appropriate initial rotational level. The rapid rise in these rotational excitation cross sections near threshold is reminiscent of the electron excitation of rotational levels of  $H_2$  via the electric quadrupole moment.<sup>32</sup>

The vibrational-excitation cross sections shown in Fig. 1 are obtained from the theory of Gentry and Giese<sup>33</sup> for energies from 6 to 1000 eV and confirmed by Schinke<sup>34</sup> for energies from 15 to 300 eV. Linder<sup>30</sup> gives similar values at energies between 6.8 and 15 eV. Relative cross sections for various final vibrational states at 30 eV have been reported recently by Niedner *et al.*<sup>35</sup> The cross sections of Fig. 1 rise and fall somewhat slower with energy than those recommended by Janev *et al.*<sup>17</sup> The experimental results of Herrero and Doering<sup>36</sup> are much smaller than the data shown, particularly at low energies. As shown in Sec. 3.2, vibrational excitation is a significant momentum- and energy-loss process for  $H^+$  in  $H_2$  at energies between 10 and 100 eV.

The cross sections for charge transfer to form  $H_2^+$  and fast H, shown in Fig. 1 for energies from the threshold 2.7 eV–4 eV, are a compromise based on several experiments. The sharp increase in cross section near threshold reported by Holliday, Muckerman, and Friedman<sup>37</sup> is supported by the rough consistency of their data for  $H^+$  on  $D_2$  to form  $D_2^+$  and  $HD^+$  with that found by Ochs and Teloy.<sup>38</sup> However, this same comparison suggests that the cross section for  $H_2^+$  formation decreases much less rapidly with increasing  $H^+$  energy than found by Holliday, Muckerman, and Friedman.<sup>37</sup> We have adopted a smooth curve, which is about 60% of the Baer *et al.*<sup>39</sup> value at 30 eV, and which approaches the results of Holliday, Muckerman, and Friedman<sup>37</sup> at energies below 5 eV and those of Gealy and Van Zyl<sup>40</sup> for  $63 < \epsilon_L < 2000$  eV. Our cross section is reasonably consistent with the low-energy portion of the cross sections for slow ion production, found by Cramer<sup>29</sup> and by Koopman.<sup>41</sup> For energies from 2 to 10 keV, our recommended values approach the tabulated values for fast H production from Barnett *et al.*<sup>15</sup> and at near 10 keV are slightly lower than the results of Rudd *et al.*<sup>42</sup> The cross section for fast H formation at 1500 eV is in good agreement with the angular integrated differential cross section data of Smith *et al.*<sup>27</sup> We assume that slow  $H^+ + H^-$  formation has not been reported. Note that  $H_2^+$  formed by charge transfer at 30 eV has a high degree of vibrational excitation.<sup>35</sup>

The excitation cross sections shown in Fig. 1 for the Lyman- $\alpha$  line are from Van Zyl *et al.*<sup>43</sup> and Van Zyl, Gealy, and Neumann<sup>44</sup> for energies from 170 eV to above 1000 eV. Note that these Lyman- $\alpha$  cross sections are almost an order of magnitude lower than those of Ottinger and Yang<sup>45</sup> for the common energy range of  $170 < \epsilon_L < 250$  eV. The excitation cross section for the Balmer- $\alpha$  (labeled as  $H\alpha$ ) line in Table 1 is from Williams, Geddes, and Gilbody<sup>46</sup> for energies above 1.5 keV and is extrapolated to lower energies as

shown. Most of the Lyman- $\alpha$  and Balmer- $\alpha$  production at  $2 < \epsilon_L < 10$  keV is Doppler shifted from the unperturbed line and so is interpreted as "projectile excitation".<sup>46</sup> The production of excited H has been observed by Hess<sup>47</sup> at  $300 < \epsilon_L < 3000$  eV for  $n^* = 3$  and 4 and by McFarland and Futch<sup>48</sup> for  $\epsilon_L > 5$  keV and  $n^* > 11$ , where  $n^*$  is the principal quantum number. If, as found by these authors for the higher  $n^*$ , one assumes that the excitation of the higher states of H varies as  $(n^*)^{-3}$ , then the sum of the excitation cross sections for H is 2.1 times the cross section for  $H(n^* = 3)$  excitation. No cross sections have been found for excitation of  $H_2$  molecular emission by  $H^+$  at energies below 20 keV. See, for example, Thomas<sup>49</sup> and Dunn, Geballe, and Pretzer.<sup>50</sup> The cross sections for excitation of the Lyman bands in the far UV are comparable with those for excitation of Lyman- $\alpha$  at 50 keV, but decrease more rapidly as the  $H^+$  energy is decreased.<sup>51</sup> There are seemingly conflicting statements as to whether or not  $H^+ - H_2$  collisions produce significant visible molecular emission.<sup>51,52</sup> There appear to be no cross-section data for  $H_2$  dissociation into ground-state H atoms in  $H^+ - H_2$  collisions.

The electron production cross sections from 400 to 10 000 eV are from Rudd *et al.*<sup>53</sup> These data were extrapolated to lower energies using the empirical formula given by these authors. At energies below 10 keV these cross sections are much smaller than those tabulated by Barnett *et al.*,<sup>15</sup> and somewhat smaller than those of Green and McNeal<sup>12</sup> and of Janev *et al.*<sup>17</sup> We assume that each electron-production event results in single ionization of the target, but with an unknown ratio  $H^+$  to  $H_2^+$ .

### 3.2. Energy, Momentum Loss, and Stopping Power for $H^+$ in $H_2$

In order to test the usefulness of the cross section set for  $H^+$  and  $H_2$  described in Sec. 3.1, we will compare the energy- and momentum-loss functions derived from the cross sections with (i) energy-loss theory developed to describe a beam of  $H^+$  traversing  $H_2$  and (ii) measurements of the drift velocity of  $H^+$  in  $H_2$  under the influence of a uniform electric field (Sec. 3.3). We will first define the loss functions and then make the comparisons.

Figure 2 and Table 2 show the energy-loss functions  $L_e(\epsilon_L)$  and momentum loss functions  $L_m(\epsilon_L)$  for  $H^+$  in  $H_2$  calculated using the cross sections of Fig. 1. In this report we will not review the fluid or moment models of ion motion leading to these quantities, but will simply define them. For a general discussion of such models, as applied to ion transport, see Kumar, Skullerud, and Robson.<sup>54</sup> The application of these quantities to a simplified model of electron motion at very high  $E/n$  has been discussed by Phelps, Jelenković, and Pitchford.<sup>55</sup> The energy-loss function used here is defined as

$$L_e(\epsilon_L) = - \frac{2Mm}{(M+m)^2} \epsilon_L Q_m(\epsilon_L) + \sum_T \epsilon_L Q'_o(\epsilon_L) + \langle \epsilon \rangle_i Q'_o(\epsilon_L). \quad (1)$$

Here  $m$  and  $M$  are the mass of the  $H^+$  and of the  $H_2$ , and  $Q'_o$

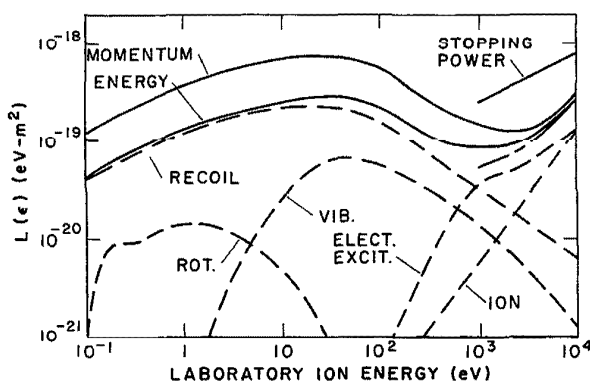


FIG. 2. Energy loss  $L_\epsilon$  and momentum loss  $L_m$  coefficients for  $H^+$  in  $H_2$  versus  $H^+$  laboratory energy. The solid curves show the total loss coefficients defined by Eqs. (1) and (3) from 0.1 eV to 10 keV. The dashed curves show the contributions resulting from elastic recoil (RECOIL), rotational excitation (ROT.), vibrational excitation (VIB.), electronic excitation (ELECT. EXCIT.), and ionization (ION.). The short solid curve shows the experimental results of Phillips,<sup>63</sup> while the chain curve is the sum of the electronic excitation and ionization curves. The loss coefficients for  $H^+$  in  $H_2$  are listed in Table 2.

and  $Q_o^i$  are the total cross sections for excitation of the  $k$ 'th process and for ionization. The first term on the right-hand side of Eq. (1) is the average energy loss caused by recoil of the  $H_2$  in the collision with the  $H^+$  as given by McDaniel.<sup>56</sup> The second term is an approximation to the energy loss in the various excitation processes discussed earlier in this section. This approximation assumes that the energy loss  $\epsilon_k$  is small compared to the  $H^+$  energy  $\epsilon_L$  as in the "continuous energy loss" models. See, for example, Porter and Green.<sup>57</sup> A similar approximation is used for the last term, i.e., the ionization term, except that  $\langle \epsilon \rangle_i$  is the average energy lost by the  $H^+$  in the ionizing collision. Rudd<sup>58</sup> has found that the average energy of electrons produced in  $H^+ + H_2$  collisions is  $\langle \epsilon \rangle_i = 0.07(\epsilon_L)^{1/2}$  eV for energies from 5 to 200 keV, where  $\epsilon_L$  is in eV. This energy loss is a minimum value, since it contains no allowance for the vibrational excitation of  $H_2^+$  or for the energy of the  $H^+$  and H fragments produced along with the electron. We also have no information on the relative yields of atomic and molecular products resulting from  $H_2$  ionization by  $H^+$ . We will assume that for  $23.1 < \epsilon_L < 10^4$  eV,

$$\langle \epsilon \rangle_i = 0.07(\epsilon_L - 23.1)^{1/2} \text{ eV.} \quad (2)$$

The dashed curves of Fig. 2 show the contributions of the elastic and various inelastic processes discussed previously in this section to  $L_\epsilon(\epsilon_L)$  and  $L_m(\epsilon_L)$ . In calculating the contribution of excitation to the highly excited states of H, we assume that the excitation of these levels is proportional to  $(n^*)^{-3}$ , where  $n^*$  is the principal quantum number, and that the observed emission cross sections are approximately equal to the state-excitation cross sections. We have neglected the energy loss due to large changes in the rotational quantum number that occur<sup>59</sup> at high  $\epsilon_L$ . Note particularly

the much smaller contribution of ionization to  $L_\epsilon(\text{tot})$  than in our earlier estimate as cited by Inokuti and Berger.<sup>23</sup> The solid curve marked "ENERGY" shows the values of  $L_\epsilon(\epsilon_L)$  obtained by summing the dashed curves.

Figure 2 provides a comparison of theoretical values of the stopping power for  $H^+$  in  $H_2$  with our calculated values of  $L_\epsilon$ . The upper solid curve between 1 and 10 keV shows theoretical values of the stopping power for  $H^+$  in  $H_2$ , calculated under the conventional assumption that they are twice the theoretical values for  $H^+$  in H.<sup>60</sup> The values from the compilation by Janni<sup>61</sup> are higher by almost 50% at  $\epsilon_L = 1$  keV, i.e., they differ by about the estimated combined uncertainties. Since the stopping power theory cited does not include the effects of angular scattering,<sup>62</sup> we have shown by the chain curve, the sum of the contributions of the various inelastic processes of Fig. 1 to  $L_\epsilon$ . Note that the disagreement of a factor of 5 at 1 keV, between our calculation and the theory shown in Fig. 2, is significantly larger than in our preliminary comparison, as cited by Inokuti and Berger,<sup>23</sup> primarily because of the much lower contribution of ionization to the energy loss. Inokuti and Berger<sup>23</sup> suggest that errors (or omissions) in the inelastic cross sections are responsible for the discrepancy with theory. If the stopping-power theory is correct at these low energies, a cross section for the electronic excitation of  $H_2$  of about  $10^{-20} \text{ m}^2$  at 1 keV would be required to supply the missing energy loss. This excitation could lead to, as yet, unmeasured processes such as dissociation into ground-state H atoms,  $H_2$  molecular emission, etc. In addition, the energy loss to dissociation during ionization could be much larger than that given up to the electrons according to Eq. (2).

Energy-loss experiments at  $\epsilon_L < 50$  keV, in which the energy of  $H^+$  is measured after a large number of collisions with  $H_2$ , such as that of Phillips,<sup>63</sup> are insensitive to the energy-loss rates for  $H^+$  in  $H_2$  because<sup>64</sup> the projectile spends about 90% of its time in the form of H and because the rate of energy loss by  $H^+$  is comparable with that for H. Thus in these energy-loss experiments and at  $\epsilon_L < 50$  keV the change of kinetic energy of the H should be regarded primarily as an indicator of the kinetic energy loss of the H and not of the energy loss of the  $H^+$ . We will see in Sec. 6.2 that the rate of energy loss by H in  $H_2$  calculated from our cross sections satisfactorily accounts for the energy-loss measurements of Phillips.<sup>63</sup>

The total momentum-loss function  $L_m(\epsilon_L)$  is defined by

$$L_m(\epsilon_L) = \frac{2M}{(m+M)} \epsilon_L Q_m(\epsilon_L) + \sum_k \epsilon_k Q_o^k(\epsilon_L) + \langle \epsilon \rangle_i Q_o^i(\epsilon_L). \quad (3)$$

Values of  $L_m(\epsilon_L)$  for  $H^+$  in  $H_2$  are shown by the solid curve marked "MOMENTUM" and are given in Table 2. Note that the only change in the momentum-loss function defined by Eq. (3) from that for energy loss defined by Eq. (1) is in the mass-dependent coefficient of the recoil term, i.e., the first term on the right-hand side. In the present case, this change increases the contribution of momentum-transfer collisions to  $L_m$  by a factor of 3 relative to that for  $L_\epsilon$  and

Table 2. Energy and momentum loss functions for  $H^+ + H_2$  tabulated by process  
(Loss in units of  $10^{-20} \text{ eV m}^2$ )

| Lab. ion<br>Energy<br>eV | Process              |                   |                   |                   |                   |                   |                      |                   |
|--------------------------|----------------------|-------------------|-------------------|-------------------|-------------------|-------------------|----------------------|-------------------|
|                          | $L_c(\text{recoil})$ | $L_c(\text{rot})$ | $L_c(\text{vib})$ | $L_c(\text{exc})$ | $L_c(\text{ion})$ | $L_c(\text{tot})$ | $L_m(\text{recoil})$ | $L_m(\text{tot})$ |
| 0.100                    | 4.000                | 0.143             |                   |                   |                   | 4.143             | 12.000               | 12.143            |
| 0.133                    | 4.682                | 0.494             |                   |                   |                   | 5.176             | 14.046               | 14.540            |
| 0.178                    | 5.374                | 0.872             |                   |                   |                   | 6.246             | 16.123               | 16.995            |
| 0.237                    | 6.113                | 0.909             |                   |                   |                   | 7.022             | 18.339               | 19.247            |
| 0.316                    | 7.098                | 0.948             |                   |                   |                   | 8.046             | 21.293               | 22.241            |
| 0.422                    | 8.153                | 1.069             |                   |                   |                   | 9.222             | 24.458               | 25.527            |
| 0.562                    | 9.372                | 1.206             |                   |                   |                   | 10.578            | 28.117               | 29.323            |
| 0.750                    | 10.599               | 1.332             |                   |                   |                   | 11.930            | 31.796               | 33.127            |
| 1.000                    | 11.811               | 1.403             | 0.020             |                   |                   | 13.334            | 35.733               | 37.157            |
| 1.334                    | 13.750               | 1.411             | 0.045             |                   |                   | 15.206            | 41.250               | 42.706            |
| 1.778                    | 14.938               | 1.341             | 0.112             |                   |                   | 16.390            | 44.813               | 46.265            |
| 2.37                     | 16.231               | 1.252             | 0.237             |                   |                   | 17.719            | 48.692               | 50.181            |
| 3.16                     | 17.890               | 1.107             | 0.461             |                   |                   | 19.558            | 53.970               | 55.537            |
| 4.22                     | 18.929               | 0.946             | 0.756             |                   |                   | 20.631            | 56.788               | 58.490            |
| 5.62                     | 19.994               | 0.777             | 1.169             |                   |                   | 21.941            | 59.983               | 61.929            |
| 7.50                     | 20.997               | 0.616             | 1.778             |                   |                   | 23.392            | 62.991               | 65.386            |
| 10.00                    | 21.778               | 0.469             | 2.522             |                   |                   | 24.769            | 65.333               | 68.325            |
| 13.34                    | 22.522               | 0.342             | 3.480             |                   |                   | 26.344            | 67.565               | 71.387            |
| 17.78                    | 22.920               | 0.223             | 4.589             |                   |                   | 27.731            | 68.760               | 73.571            |
| 23.7                     | 22.976               | 0.137             | 5.617             |                   |                   | 28.730            | 68.928               | 74.682            |
| 31.6                     | 22.487               | 0.077             | 6.391             |                   |                   | 28.955            | 67.462               | 73.929            |
| 42.2                     | 21.553               |                   | 6.676             |                   |                   | 28.229            | 64.660               | 71.334            |
| 56.2                     | 20.744               |                   | 6.527             |                   |                   | 27.271            | 62.232               | 68.759            |
| 75.0                     | 18.664               |                   | 6.041             | 0.012             | 0.016             | 24.733            | 55.992               | 62.061            |
| 100.0                    | 16.667               |                   | 5.583             | 0.050             | 0.027             | 22.326            | 50.000               | 55.660            |
| 133.4                    | 14.224               |                   | 4.987             | 0.086             | 0.040             | 19.348            | 42.673               | 47.796            |
| 177.8                    | 11.065               |                   | 4.421             | 0.104             | 0.060             | 15.740            | 33.195               | 37.670            |
| 237.                     | 8.642                |                   | 3.788             | 0.363             | 0.089             | 12.883            | 25.927               | 30.167            |
| 316.                     | 7.168                |                   | 3.173             | 0.626             | 0.128             | 11.095            | 21.503               | 25.431            |
| 422.                     | 5.997                |                   | 2.616             | 1.089             | 0.183             | 9.885             | 17.992               | 21.880            |
| 562.                     | 4.874                |                   | 2.140             | 1.772             | 0.276             | 9.062             | 14.621               | 18.809            |
| 750.                     | 3.899                |                   | 1.692             | 2.687             | 0.398             | 8.676             | 11.698               | 16.474            |
| 1000.                    | 3.200                |                   | 1.367             | 3.530             | 0.580             | 8.678             | 9.600                | 15.077            |
| 1334.                    | 2.667                |                   | 1.070             | 4.136             | 0.861             | 8.734             | 8.001                | 14.068            |
| 1778.                    | 2.134                |                   | 0.827             | 4.573             | 1.265             | 8.799             | 6.402                | 13.066            |
| 2371.                    | 1.739                |                   | 0.633             | 4.870             | 1.842             | 9.183             | 5.217                | 12.661            |
| 3162.                    | 1.405                |                   | 0.465             | 5.775             | 2.705             | 10.351            | 4.216                | 13.162            |
| 4217.                    | 1.162                |                   | 0.347             | 7.231             | 3.987             | 12.726            | 3.486                | 15.050            |
| 5623.                    | 0.950                |                   | 0.256             | 8.920             | 5.779             | 15.905            | 2.849                | 17.805            |
| 7499.                    | 0.783                |                   | 0.182             | 10.909            | 8.581             | 20.455            | 2.350                | 22.021            |
| 10000.                   | 0.644                |                   | 0.131             | 13.580            | 12.316            | 26.671            | 1.833                | 27.960            |

accounts for the difference in the solid curves of Fig. 2. In deriving Eq. (3) we assumed that the inelastic-scattering cross sections are strongly peaked in the forward direction so that the momentum loss can be expressed in terms of the energy loss.<sup>65</sup> Although this assumption will fail at low energies, the loss functions for inelastic excitation are small enough so that the error in  $L_m(\epsilon_L)$  can be neglected.

### 3.3. Drift Velocities and Reaction Coefficients for $H^+$ in $H_2$

Our second test of the usefulness of the cross section set in Fig. 1 is a comparison of calculated and measured drift velocities  $W$  for  $H^+$  in  $H_2$ . Figure 3 and Table 3 show comparisons of calculated and experimental<sup>66</sup> values of the drift velocity of  $H^+$  in  $H_2$  for high values of  $E/n$ , the ratio of the electric field to the gas density. The calculated drift velocities were obtained by modifying the single-beam models of electron motion derived by Phelps, Jelenković, and Pitchford<sup>55</sup> so as to apply to ion motion. The only changes to the energy- and momentum-balance models for electrons are to replace the elastic scattering terms for electrons by the first terms on the right-hand sides of Eqs. (1) and (3), respectively. Therefore the  $H^+$  drift energies and velocities are found by solving the steady-state forms of the momentum balance

$$\frac{eE}{n} = L_m(\epsilon_m) + 2\epsilon_m Q_D^i(\epsilon_m), \quad (4)$$

or the energy balance

$$\frac{eE}{n} = L_\epsilon(\epsilon_\epsilon) + \epsilon_\epsilon Q_D^i(\epsilon_\epsilon). \quad (5)$$

Here  $\epsilon_m$  and  $\epsilon_\epsilon$  are the laboratory energies of the  $H^+$  ions drifting through  $H_2$  as calculated using the momentum and energy balance approximations, respectively. In either case the  $H^+$  drift velocity  $W_{m,\epsilon}(H^+)$  is calculated using

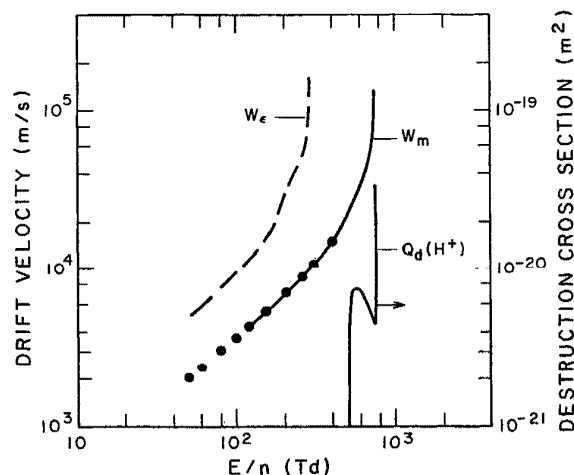


FIG. 3. Drift velocities  $W_\epsilon$  and  $W_m$  and effective destruction cross section  $Q_d$  for  $H^+$  in  $H_2$  vs  $E/n$ . The solid curves were calculated using the momentum balance model of Eq. (4), while the dashed curve was calculated using the energy balance model of Eq. (5). The points are experimental drift velocities from Miller *et al.*<sup>66</sup> The calculated results are listed in Table 3.

$$W_{m,\epsilon}(H^+) = (2e\epsilon_{m,\epsilon}/m)^{1/2}. \quad (6)$$

The calculated drift velocities are shown by the curves of Fig. 3 and the experiments<sup>66</sup> are indicated by the points. We note that the values of  $W(H^+)$  from the momentum-balance model (solid curve) and the energy-balance model, (dashed curve) differ by a factor of 2 or more. Although this comparison shows that we obtain consistency with experiment by the choice of  $Q_m(\epsilon_L)$  shown in Fig. 1 and the use of the momentum-balance transport model, it does not test either

Table 3. Calculated steady-state energies and drift velocities for  $H^+$  in  $H_2$ .

| E/n<br>(Td) <sup>a</sup> | Energy balance<br>model     |                       | Momentum balance<br>model |                |                             |
|--------------------------|-----------------------------|-----------------------|---------------------------|----------------|-----------------------------|
|                          | $\epsilon_\epsilon$<br>(eV) | $W_\epsilon$<br>(m/s) | $\epsilon_m$<br>(eV)      | $W_m$<br>(m/s) | $Q_d$<br>( $10^{-20} m^2$ ) |
| 50                       | 0.13                        | 5000                  | NA <sup>b</sup>           | NA             | NA                          |
| 70                       | 0.18                        | 6000                  | NA                        | NA             | NA                          |
| 100                      | 0.5                         | 9800                  | NA                        | NA             | NA                          |
| 150                      | 1.3                         | 15800                 | 0.14                      | 5200           | 0                           |
| 200                      | 4.5                         | 29500                 | 0.26                      | 7100           | 0                           |
| 280                      | 22                          | 65300                 | 0.51                      | 9900           | 0                           |
| 300                      | runaway                     |                       | 0.6                       | 10800          | 0                           |
| 400                      |                             |                       | 1.2                       | 15000          | 0                           |
| 500                      |                             |                       | 2.2                       | 21000          | 0                           |
| 600                      |                             |                       | 5.4                       | 32000          | 0.72                        |
| 700                      |                             |                       | 13                        | 50000          | 0.52                        |
| 730                      |                             |                       | 20                        | 62000          | 0.46                        |
| 750                      |                             |                       | runaway                   |                | > 1                         |

<sup>a</sup> 1 Td =  $10^{-21}$  V m<sup>2</sup>.

<sup>b</sup> NA means not available because the steady-state energy  $\epsilon_m$  is less than 0.1 eV, the minimum energy for which cross section data were assembled.

of them separately. In other words, the values of  $Q_m$  shown by the solid curve in Fig. 1 are somewhat uncertain because of approximations made in the single-beam, momentum-balance model of  $H^+$  motion and the low-energy  $Q_m$  values could be improved by the use of a more accurate model<sup>56</sup> to fit the data. We estimate the uncertainty in  $Q_m$  for  $0.1 < \epsilon_L < 1$  eV due to the approximations of momentum-balance model to be  $< 20\%$ . This uncertainty is illustrated in Fig. 1 by the differences between the solid  $Q_m(\epsilon)$  curve and the long-dashed lines representing extrapolations to higher energies of the constant cross section and the constant collision frequency derived using accurate drift velocity models<sup>56</sup> fitted to thermal  $H^+$  mobility data for 300 K. Note that a good fit to the experimental drift velocity data can be obtained using the energy-balance model only by increasing the  $Q_m(c)$  values in Fig. 1, by a factor of 3. We consider such values of  $Q_m$  unrealistic and have not shown the results.

The momentum-balance calculations predict runaway, i.e., a failure of the  $H^+$  to reach a steady-state drift motion,<sup>67</sup> when  $E/n$  exceeds the maximum value of  $L_m(\epsilon_L) = 735 \times 10^{-21} \text{ V m}^2$  at  $\epsilon_L \approx 30$  eV. We suggest that runaway of some of the  $H^+$  ions is responsible for the increase of the measured  $H^+$  normalized mobility at  $E/n \geq 300 \text{ Td}$ ,<sup>66</sup> where for any ion the normalized mobility is defined by  $\mu n = W/(E/n)$ . The  $E/n$  for runaway shown in Fig. 3, which is calculated using the single-beam, energy-balance model using the cross sections of Fig. 1, is well above that for which drift velocity data is available.

Figure 3 and Table 3 also show the cross sections for  $H^+$  destruction  $Q_d$ , as given by the single-beam, momentum-balance model using our cross section set. In this simple model,  $Q_d$  is the cross section for  $H_2^+$  formation at the energy of the  $H^+$  beam. We see from Fig. 3 that the destruction cross section increases rapidly at  $E/n$  just above the highest  $E/n$  values for which drift velocity measurements were reported.<sup>66</sup> Note that the energy-balance model predicts rapid destruction at  $E/n$  well below those for which drift-velocity data were measured.<sup>66</sup> Also, the predicted ionization coefficient is negligibly small for  $E/n$ , for which equilibrium is attained.

The steady-state results of Fig. 3 and Table 3 are not applicable in some discharge models because there are an insufficient number of collisions for the  $H^+$  ions to reach equilibrium motion or because the  $E/n$  is high enough so that runaway occurs. In such cases it is necessary to use the appropriate spatial and/or time dependent approximations to the Boltzmann equation for the ions and the electrons. Such models have been applied to  $H_2$  discharges by a number of workers using older cross section sets.<sup>1,7,68,69</sup> Completely analytic models are represented by the work of Pustynskii and Shumilin.<sup>70</sup>

## 4. $H_2^+$ Collisions with $H_2$

### 4.1. $H_2^+ - H_2$ Cross Sections

The dominant cross section for low-energy  $H_2^+$  in  $H_2$  is that for the formation of  $H_3^+ + H$ . The cross section for this process shown in Fig. 4 is based on that of Neynaber and Trujillo.<sup>71</sup> Although the energy dependence is consistent

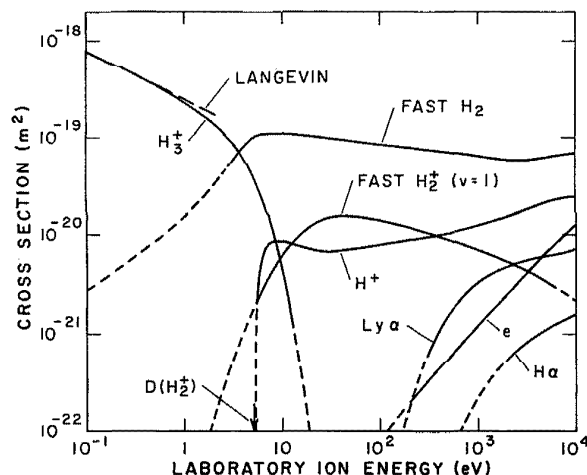


FIG. 4. Cross sections for collisions of  $H_2^+$  with  $H_2$  versus laboratory energy of  $H_2^+$  for  $H_2$  at rest. The solid curves are based on experiment or theory while the short-dashed curves are extrapolations or interpolations. The curves show cross sections for  $H_3^+$  formation; charge transfer to form slow  $H_2^+$  and fast  $H_2$ ; dissociation to  $H^+$ ; Ly- $\alpha$  and H $\alpha$  excitation; and electron production ( $e$ ). These cross sections are listed in Table 4. The arrow shows the laboratory energy required for dissociation of  $H_2^+$ .

with that of Giese and Maier,<sup>72</sup> the magnitude is considerably smaller than theirs. The cross sections shown are also smaller than those of Shao and Ng,<sup>73</sup> particularly at energies above 2 eV. The adopted cross sections are consistent with the spiraling limit of the polarization-interaction model.<sup>56</sup> These cross sections agree with the recommendations of Janev *et al.*<sup>17</sup> and Tawara *et al.*<sup>18</sup> These and other cross sections adopted for  $H_2^+$  in  $H_2$  are tabulated in Table 4.

The charge transfer cross section, i.e., the cross section for the formation of slow  $H_2^+$ , shown in Fig. 4 for energies from 5 to 400 eV is taken from Barnett *et al.*<sup>15</sup> At energies above 2 keV the cross section is from Latimer, Browning, and Gilbody.<sup>74</sup> At energies below 5 eV our charge-transfer cross section decreases with decreasing energy as recommended by Tawara *et al.*<sup>18</sup> because of competition with  $H_3^+$  formation. This decrease differs from that recommended by Janev *et al.*<sup>17</sup> The cross section for the destruction of fast  $H_2^+$  is slightly larger<sup>74</sup> than that shown for charge transfer at energies from 1 to 20 keV.

We have found no information on the rotational excitation of  $H_2^+$  in  $H_2^+ - H_2$  collisions. However, the lack of dependence of the charge-transfer cross sections on the initial rotational state<sup>75</sup> of the  $H_2^+$  suggests that one assume that the product  $H_2^+$  has the rotational distribution of the target  $H_2$ . Also, experiments with 800 eV  $N_2^+$  in  $N_2$  indicate that the rotational excitation of the product  $N_2^+$  produced in charge-transfer collisions is small in spite of large vibrational excitation.<sup>76</sup> In these experiments the fast  $N_2^+$  product was rotationally excited in inelastic collisions without charge transfer.

The vibrational excitation and deexcitation of  $H_2^+$  in

Table 4. Cross sections for  $H_2^+ + H_2$  collisions tabulated by product(s).  
(Cross sections in units of  $10^{-20} \text{ m}^2$ )

| Lab. ion<br>energy<br>eV | Product     |              |                     |           |             |            |        |
|--------------------------|-------------|--------------|---------------------|-----------|-------------|------------|--------|
|                          | $H_3^+ + H$ | slow $H_2^+$ | $v=0 \rightarrow 1$ | $H^+ + H$ | Ly $\alpha$ | H $\alpha$ | e      |
| 0.10                     | 78          | 0.28         |                     |           |             |            |        |
| 0.1334                   | 68          | 0.34         |                     |           |             |            |        |
| 0.1778                   | 59          | 0.43         |                     |           |             |            |        |
| 0.237                    | 51          | 0.49         |                     |           |             |            |        |
| 0.316                    | 44          | 0.60         |                     |           |             |            |        |
| 0.422                    | 38          | 0.75         |                     |           |             |            |        |
| 0.562                    | 32.5        | 0.95         |                     |           |             |            |        |
| 0.750                    | 27          | 1.19         |                     |           |             |            |        |
| 1.00                     | 22.7        | 1.53         |                     |           |             |            |        |
| 1.334                    | 18.7        | 2.03         |                     |           |             |            |        |
| 1.778                    | 15.3        | 2.6          | 0.0085              |           |             |            |        |
| 2.37                     | 11.8        | 4.1          | 0.0245              |           |             |            |        |
| 3.16                     | 8.4         | 5.9          | 0.057               |           |             |            |        |
| 4.22                     | 5.4         | 8.5          | 0.119               |           |             |            |        |
| 5.62                     | 2.9         | 10.4         | 0.225               | 0.33      |             |            |        |
| 7.50                     | 1.3         | 11.0         | 0.395               | 0.83      |             |            |        |
| 10.0                     | 0.42        | 10.8         | 0.63                | 0.85      |             |            |        |
| 13.34                    | 0.093       | 10.6         | 0.85                | 0.78      |             |            |        |
| 17.78                    | 0.015       | 10.2         | 1.12                | 0.72      |             |            |        |
| 23.7                     |             | 9.9          | 1.36                | 0.68      |             |            |        |
| 31.6                     |             | 9.6          | 1.49                | 0.67      |             |            | 0.0001 |
| 42.2                     |             | 9.2          | 1.52                | 0.69      |             |            | 0.0008 |
| 56.2                     |             | 8.9          | 1.49                | 0.70      |             |            | 0.0021 |
| 75.0                     |             | 8.6          | 1.43                | 0.74      |             |            | 0.0048 |
| 100                      |             | 8.4          | 1.36                | 0.78      |             |            | 0.0084 |
| 133.4                    |             | 8.2          | 1.30                | 0.82      |             |            | 0.012  |
| 177.8                    |             | 7.9          | 1.20                | 0.86      | 0.013       |            | 0.017  |
| 237                      |             | 7.7          | 1.12                | 0.91      | 0.033       |            | 0.024  |
| 316                      |             | 7.4          | 1.03                | 0.95      | 0.068       |            | 0.0335 |
| 421                      |             | 7.2          | 0.94                | 1.01      | 0.12        |            | 0.047  |
| 562                      |             | 7.1          | 0.86                | 1.08      | 0.183       |            | 0.064  |
| 750                      |             | 6.8          | 0.78                | 1.15      | 0.255       | 0.0133     | 0.091  |
| 1000                     |             | 6.4          | 0.71                | 1.24      | 0.325       | 0.0233     | 0.124  |
| 1334                     |             | 6.2          | 0.64                | 1.34      | 0.39        | 0.034      | 0.17   |
| 1778                     |             | 5.9          | 0.57                | 1.48      | 0.44        | 0.049      | 0.23   |
| 2371                     |             | 5.9          | 0.50                | 1.62      | 0.50        | 0.064      | 0.31   |
| 3162                     |             | 5.9          | 0.44                | 1.82      | 0.55        | 0.081      | 0.41   |
| 4217                     |             | 6.1          | 0.37                | 1.98      | 0.58        | 0.099      | 0.55   |
| 5623                     |             | 6.4          | 0.31                | 2.2       | 0.62        | 0.119      | 0.73   |
| 7499                     |             | 6.8          | 0.26                | 2.38      | 0.64        | 0.138      | 0.95   |
| 10000                    |             | 7.0          | 0.215               | 2.44      | 0.72        | 0.157      | 1.27   |

collisions with  $H_2$  is a potentially important process in  $H_2$  discharges at high  $E/n$  because of the possible effect of vibrational excitation on the cross section for dissociation<sup>77,78</sup> of  $H_2^+$ . In Fig. 4 we have adopted an energy dependence of the relative cross sections that is approximately that of Bates and Ried,<sup>79</sup> but relative magnitudes that are closer to the experiments by Liao and Ng<sup>80</sup> for  $8 < \epsilon_L < 32$  eV and the average of the theoretical values of Lee and DePristo for  $800 < \epsilon_L < 1000$  eV. These values are normalized to the total charge-exchange cross section of Fig. 4. The absolute charge-transfer and vibrational-excitation cross sections of Lee and DePristo<sup>81</sup> decrease much more rapidly with energy, for energies near 1 keV, than those shown in Fig. 4. The deexcitation cross section for  $H_2^+$  ( $v=1$ ) obtained at 600 eV by Herrero and Doering<sup>82</sup> is about an order of magnitude smaller than the cross sections shown. The production of vibrationally excited  $H_2$  is not shown or tabulated, but according to Bates and Ried<sup>79</sup> and Moran and Flannery,<sup>83</sup> the cross sections are comparable with those for the production

of vibrationally excited  $H_2^+$ . The absolute cross section for vibrational excitation of  $H_2$  from experiments at energies in the 100–500 eV range by Moore and Doering<sup>84</sup> is about a factor of 5 below the theoretical values. Vibrational excitation has not been included in previous compilations.

The cross sections shown in Fig. 4 for the formation of  $H^+$  in  $H_2^+ + H_2$  collisions are from Zurkin *et al.*<sup>85</sup> for energies from 100 to 2000 eV, and (for fast  $H^+$  formation) from McClure<sup>86</sup> for energies from 3.3 to 10 keV. For energies from threshold at 5.4 to 10 eV we have used the energy dependence of Moran and Roberts,<sup>87</sup> but with the data shifted to the expected threshold. This shift is supported by the observation of the expected threshold for dissociation in the  $D_2^+ + HD$  reaction by Anderson *et al.*<sup>88</sup> Our low-energy recommendation is also consistent with Tunitskii *et al.*<sup>89</sup> and Guyon *et al.*<sup>78</sup> Guyon *et al.* conclude from their experiments that a large fraction of the dissociation products are  $H^+ + H$  with low relative velocities in the center-of-mass system. This conclusion has been questioned by Eaker and

Schatz.<sup>90</sup> Cross sections for the formation of slow  $H^+$  are reported by Latimer *et al.*<sup>74</sup> for  $4 < \epsilon_L < 100$  keV.

Data showing a strong dependence of the cross section for collisional dissociation of  $H_2^+$  on the degree of vibrational excitation have been obtained by Guyon *et al.*<sup>78</sup> at  $\epsilon_L$  of 8 to 32 eV and by Lindsay, Yousif, and Latimer<sup>77</sup> at 1 keV. Eaker and Schatz<sup>90</sup> confirm theoretically this dependence on the initial vibrational state. Guyon *et al.*<sup>78</sup> suggest that these results may explain why the cross sections for  $H^+$  formation at low ion energies found by Vance and Bailey<sup>91</sup> using 80-eV electrons to produce the  $H_2^+$  are much larger than those obtained using techniques which form  $H_2^+$ , in known vibrational levels. The potential importance of vibrationally excited  $H_2^+$  in models of  $H_2$  discharges is increased by the fact that it is also formed in  $H^+ + H_2$  collisions,<sup>35</sup> and in  $H_2^+ + H_2$  charge transfer collisions.<sup>80</sup>

The Lyman- $\alpha$  cross sections are from Dunn, Geballe, and Pretzer<sup>50</sup> for energies from 300 to 3000 eV and from Van Zyl *et al.*<sup>43</sup> for energies up to 25 keV. The Balmer- $\alpha$  cross sections are from Williams *et al.*<sup>46</sup> for energies above 2000 eV and show an increase in the fraction resulting in fast-excited H atoms with increasing energy. The short-dashed sections of the curves, show extrapolations of the experimental data. We have found no published information<sup>49</sup> regarding the excitation of  $H_2$  molecular spectra by  $H_2^+$ . One reason for failure to detect  $H_2$  band and continuum emission is its wide-spectral range and resultant relatively weak signals from the high spectral-resolution detection systems used for measurement of emission from H atoms.

The electron production cross sections shown in Fig. 4 are from apparently unpublished results of Sataka *et al.* cited by Tawara *et al.*<sup>18</sup> for energies above 200 eV. At  $5 < \epsilon_L < 100$  keV these data are slightly below those recommended by Barnett *et al.*<sup>15</sup> However, the cross sections at low energies are much smaller than the Barnett *et al.* values. Again, we expect that electron production is accompanied by the formation of  $H_2^+$  and  $H^+$ . The ratio of  $H^+$  to  $H_2^+$  is unknown in the  $\epsilon_L$  range of interest.

#### 4.2. Drift Velocities and Reaction Coefficients for $H_2^+$ in $H_2$

There appear to be no measurements of the drift velocity of  $H_2^+$  in  $H_2$  against which to test our cross section set. This lack of data is to be expected for low  $E/n$  because of the dominance of the cross section for  $H_3^+$  formation over that for charge transfer for  $\epsilon_L < 3$  eV. We must therefore rely on theory to predict the ion behavior under swarm conditions. Since the cross section for charge-transfer collisions is significantly larger than that for  $H_3^+$  formation for  $\epsilon_L > 10$  ( $E/n > 1$  kTd), the drift of  $H_2^+$  in  $H_2$  and the description of  $H_2^+ - H_2$  collisions in terms of spatial-reaction or excitation coefficients becomes meaningful at  $E/n > 1$  kTd. For  $E/n > 1$  kTd we will consider values of the gas density, times distance  $d$ , which are large enough so that the  $H_2^+$  ion motion is in equilibrium<sup>92</sup> at the applied  $E/n$  and will neglect the effect of  $H_3^+$  formation on the ion energy distribution. The drift velocity is calculated<sup>56,92</sup> using the relation

$$W^+ = (2eE/\pi mn Q_{CT})^{1/2}, \quad (7)$$

while the ion "temperature" in eV is calculated using the relation<sup>56,92</sup>

$$T_+ = E/(nQ_{CT}), \quad (8)$$

where  $Q_{CT}$  is the cross section for charge transfer collisions between  $H_2^+$  and  $H_2$ . The energy distribution of ion energies  $\epsilon_L$  in the field direction is<sup>56,92</sup>

$$F(\epsilon_L) = T_+ \exp(-\epsilon_L/T_+). \quad (9)$$

The spatial-reaction or excitation coefficient  $\alpha^k/n$  for process  $k$  calculated using this distribution function is given by<sup>9,10,55</sup>

$$\begin{aligned} \frac{\alpha^k}{n} &= \frac{\int v Q_o^k(v) f(v, \Theta) d^3v}{\int v \cos(\Theta) f(v, \Theta) d^3v} \\ &= \frac{\int_0^\infty Q_o^k(\epsilon) F(\epsilon) d\epsilon}{\int_0^\infty F(\epsilon) d\epsilon} \equiv \langle Q^k \rangle. \end{aligned} \quad (10)$$

Here  $v$  and  $\Theta$  are the magnitude and angle of the ion velocity relative to the electric field,  $f(v, \Theta)$  is the three-dimensional velocity distribution,<sup>56</sup> and  $\epsilon$  is temporarily used for the laboratory ion energy instead of  $\epsilon_L$ . Note that since  $T_+$  is a function only of  $E/n$  at the moderate and high  $E/n$  of interest, in applications of the data this section,  $\alpha^k/n$  and  $\langle Q^k \rangle$  are functions of  $E/n$ . It should be kept in mind that the equality of the spatial-reaction coefficient  $\alpha^k/n$  and the average cross section  $\langle Q^k \rangle$  is a property of the one-dimensional velocity distribution appropriate to ions at moderate to high  $E/n$  and for which charge-transfer scattering is dominant.<sup>56</sup> The calculated values of the  $H_2^+$  drift velocity and temperature are shown in Fig. 5 by the solid and dashed curves.

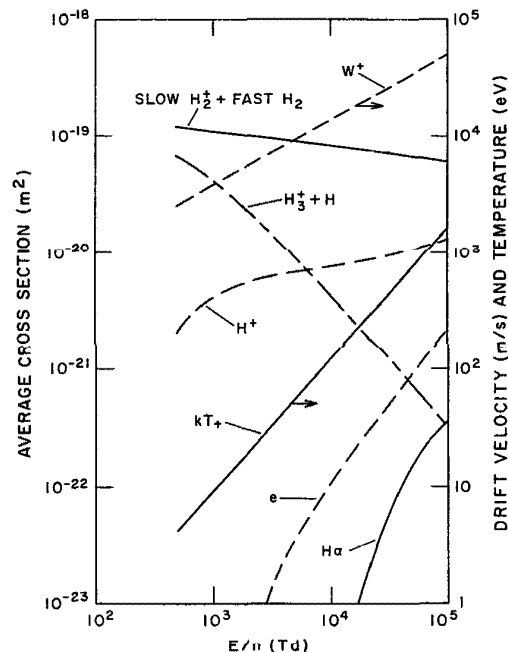


FIG. 5. Average cross sections, drift velocities  $W^+$ , and ion "temperature"  $kT_+$  as a function of  $E/n$  for  $H_2^+$  drifting through  $H_2$ . The average cross section curves are for charge transfer to form SLOW  $H_2^+$  + FAST  $H_2$ ; reaction to form  $H_3^+ + H$ ; dissociation to form  $H^+$ ; ionization to produce an electron ( $e$ ); and excitation of  $H\alpha$ . These data are listed in Table 5.

Table 5. Calculated transport coefficients and average cross sections for  $H_2^+$  in  $H_2$ .

| $E/n$<br>(Td) <sup>a</sup> | $Q_{CT}$ <sup>b</sup><br>(m <sup>2</sup> ) | $W^+$<br>(m/s) | $T_+$<br>(eV) | $\langle Q(H_3^+) \rangle$<br>(m <sup>2</sup> ) | $\langle Q(H^+) \rangle$<br>(m <sup>2</sup> ) | $\langle Q(H\alpha) \rangle$<br>(m <sup>2</sup> ) | $\langle Q_{ion} \rangle$<br>(m <sup>2</sup> ) |
|----------------------------|--|----------------|---------------|---|---|---|--|
| 1000                       | 1.1E-19 <sup>c</sup>                       | 3740           | 9.09          | 4.2E-20   | 4.1E-21                                       | 1.3E-52   | 2.5E-25  |
| 2000                       | 1.0E-19                                    | 5540           | 20            | 2.3E-20   | 5.6E-21                                       | 2.3E-37   | 4.1E-24  |
| 3000                       | 9.6E-20                                    | 6930           | 31.2          | 1.5E-20   | 6.1E-21                                       | 4.7E-32   | 1.2E-23  |
| 5000                       | 9.0E-20                                    | 9240           | 55.6          | 9.0E-21   | 6.7E-21                                       | 7.7E-28   | 3.6E-23  |
| 10000                      | 8.3E-20                                    | 13600          | 120.5         | 4.3E-21   | 7.6E-21                                       | 6.3E-25   | 1.1E-22  |
| 20000                      | 7.6E-20                                    | 20100          | 263           | 2.0E-21   | 8.7E-21                                       | 1.7E-23   | 2.8E-22  |
| 30000                      | 7.2E-20                                    | 25300          | 417           | 1.3E-21   | 9.5E-21                                       | 5.2E-23   | 4.8E-22  |
| 50000                      | 6.6E-20                                    | 34100          | 758           | 7.0E-22   | 1.1E-20                                       | 1.5E-22   | 9.3E-22  |
| 100000                     | 6.0E-20                                    | 50600          | 1667          | 3.2E-22   | 1.3E-20                                       | 3.7E-22   | 2.1E-21  |

<sup>a</sup> 1 Td =  $10^{-21}$  V m<sup>2</sup>

<sup>b</sup>  $Q_{CT}$  values used in Eqs. (7) and (8)

<sup>c</sup> 1.1E-19 means  $1.1 \times 10^{-19}$

respectively, for  $E/n > 1$  kTd. These results are tabulated in Table 5. We leave the discussion of the effects of departures from ion collisional equilibrium and of ion conversion reactions for papers concerned with applications.<sup>1,7,68,69,92</sup>

Also shown in Fig. 5 and Table 5 are calculated average cross sections or spatial-excitation coefficients  $\alpha^k/n$  obtained using Eq. (10) for some of the collision cross sections shown in Fig. 4. We note, for example, that the average cross section resulting in the production of fast  $H_2$  is about ten times that for  $H_2^+$  loss by  $H^+$  formation, so that one expects a significant production of fast  $H_2$  by the fast  $H_2^+$  drifting through  $H_2$ . The apparent ionization coefficients for  $H_2^+$  measured by Townsend and Llewellyn Jones<sup>93</sup> for 400 Td  $< E/n < 1.5$  kTd vary from  $4 \times 10^{-25}$  to  $5 \times 10^{-24}$  m<sup>2</sup>. These values are too small to be shown in Fig. 5. At  $E/n = 1$  kTd their ionization coefficient is about an order of magnitude larger than our present calculated value. Our earlier calculations<sup>22</sup> of this ionization coefficient are too high because of our use of too large an ionization cross section. The differences in calculated and experimental ionization coefficients could possibly be caused by the buildup of the  $H_2^+$  vibrational "temperature" in charge-transfer collisions. A better understanding of experimental results such as these will have to await more complete models of ion and electron motion in  $H_2$ .

## 5. $H_3^+$ Collisions with $H_2$

### 5.1. $H_3^+ - H_2$ Cross Sections

The low-energy momentum-transfer cross sections for  $H_3^+$  in  $H_2$  shown by the solid curve in Fig. 6 and Table 6 are obtained from the mobility of  $H_3^+$  in  $H_2$  as tabulated by Ellis *et al.*<sup>24</sup> and from the approximate single-beam, momentum-balance model. See Sec. 5.2 for details. The long-dashed lines show extrapolations to higher energies of fits to thermal

mobility data using accurate constant-cross-section and constant-collision-frequency models. At present we have no experimental basis for extending the solid curve to higher energies. At energies above 1000 eV the cross section shown in Fig. 6 is estimated by scaling the experimental data for  $H^+$  and H on  $H_2$  by the mass factor given by screened Coulomb theory,<sup>56</sup> i.e., by 2.8. We have then interpolated between these data for intermediate energies.

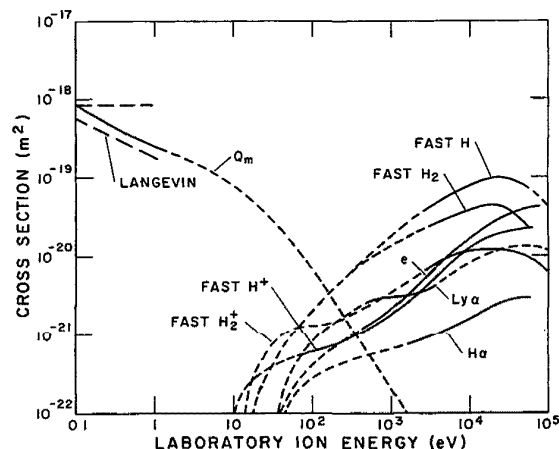


Fig. 6. Cross sections for collisions of  $H_3^+$  with  $H_2$  versus laboratory energy of  $H_3^+$  for  $H_2$  at rest. The solid curves are based on experiment or theory, while the short-dashed curves are extrapolations or interpolations. The curves show cross sections for momentum transfer  $Q_m$ ; charge transfer to form slow  $H_2^+$  and FAST H and slow  $H^+$  and FAST  $H_2$ ; dissociation to FAST  $H^+$  and FAST  $H_2^+$ ; Ly- $\alpha$  and H $\alpha$  excitation; and electron production (e). These cross sections are listed in Table 6. The long-dashed lines are extrapolations to higher energies of fits of constant cross section and constant collision-frequency models to 300 K mobility data.

Table 6. Cross sections for  $H_3^+ + H_2$  collisions tabulated by product(s).  
(Cross sections in units of  $10^{-20} \text{ m}^2$ )

| Lab. ion<br>energy<br>eV | fast $H^+$<br>(10) <sup>a</sup> | fast $H_2^+$<br>(10) | fast H<br>(11.25) | Product<br>fast $H_2$<br>(10) | Ly $\alpha$<br>(37) | H $\alpha$<br>(41.5) | e<br>(38.5) | $Q_m$   |
|--------------------------|---------------------------------|----------------------|-------------------|-------------------------------|---------------------|----------------------|-------------|---------|
| 0.10                     |                                 |                      |                   |                               |                     |                      |             | 85.     |
| 0.1334                   |                                 |                      |                   |                               |                     |                      |             | 72.5    |
| 0.1778                   |                                 |                      |                   |                               |                     |                      |             | 61      |
| 0.237                    |                                 |                      |                   |                               |                     |                      |             | 51.5    |
| 0.316                    |                                 |                      |                   |                               |                     |                      |             | 44.5    |
| 0.422                    |                                 |                      |                   |                               |                     |                      |             | 38      |
| 0.562                    |                                 |                      |                   |                               |                     |                      |             | 33.3    |
| 0.750                    |                                 |                      |                   |                               |                     |                      |             | 28.5    |
| 1.00                     |                                 |                      |                   |                               |                     |                      |             | 25.     |
| 1.334                    |                                 |                      |                   |                               |                     |                      |             | 22.6    |
| 1.778                    |                                 |                      |                   |                               |                     |                      |             | 20      |
| 2.37                     |                                 |                      |                   |                               |                     |                      |             | 17.8    |
| 3.16                     |                                 |                      |                   |                               |                     |                      |             | 15.7    |
| 4.22                     |                                 |                      |                   |                               |                     |                      |             | 13.6    |
| 5.62                     |                                 |                      |                   |                               |                     |                      |             | 11.6    |
| 7.50                     |                                 |                      |                   |                               |                     |                      |             | 9.5     |
| 10.0                     | 0.009                           |                      |                   |                               |                     |                      |             | 7.85    |
| 13.34                    | 0.0183                          |                      |                   |                               |                     |                      |             | 6.3     |
| 17.78                    | 0.026                           | 0.0283               | 0.011             | 0.011                         |                     |                      |             | 4.85    |
| 23.7                     | 0.033                           | 0.0525               | 0.0255            | 0.0255                        |                     |                      |             | 3.69    |
| 31.6                     | 0.0395                          | 0.077                | 0.044             | 0.044                         |                     |                      |             | 2.75    |
| 42.2                     | 0.045                           | 0.099                | 0.069             | 0.069                         | 0.0197              | 0.009                | 0.0123      | 2.01    |
| 56.2                     | 0.051                           | 0.117                | 0.102             | 0.102                         | 0.037               | 0.0156               | 0.0208      | 1.44    |
| 75.0                     | 0.0555                          | 0.127                | 0.149             | 0.149                         | 0.057               | 0.022                | 0.0305      | 0.99    |
| 100                      | 0.0595                          | 0.131                | 0.207             | 0.207                         | 0.082               | 0.0275               | 0.041       | 0.67    |
| 133.4                    | 0.0647                          | 0.133                | 0.283             | 0.283                         | 0.107               | 0.033                | 0.0525      | 0.44    |
| 177.8                    | 0.071                           | 0.141                | 0.383             | 0.383                         | 0.137               | 0.038                | 0.067       | 0.297   |
| 237                      | 0.08                            | 0.159                | 0.51              | 0.51                          | 0.166               | 0.043                | 0.0825      | 0.195   |
| 316                      | 0.093                           | 0.183                | 0.67              | 0.64                          | 0.20                | 0.048                | 0.10        | 0.12    |
| 422                      | 0.107                           | 0.21                 | 0.87              | 0.795                         | 0.237               | 0.0525               | 0.12        | 0.08    |
| 562                      | 0.127                           | 0.247                | 1.12              | 0.97                          | 0.273               | 0.056                | 0.143       | 0.051   |
| 750                      | 0.153                           | 0.293                | 1.43              | 1.17                          | 0.297               | 0.0605               | 0.174       | 0.0325  |
| 1000                     | 0.186                           | 0.35                 | 1.83              | 1.38                          | 0.305               | 0.065                | 0.218       | 0.0203  |
| 1334                     | 0.218                           | 0.415                | 2.28              | 1.61                          | 0.313               | 0.071                | 0.273       | 0.0124  |
| 1778                     | 0.287                           | 0.505                | 2.86              | 1.88                          | 0.327               | 0.077                | 0.35        | 0.0072  |
| 2371                     | 0.365                           | 0.61                 | 3.53              | 2.16                          | 0.347               | 0.085                | 0.47        | 0.0046  |
| 3162                     | 0.475                           | 0.73                 | 4.27              | 2.43                          | 0.40                | 0.095                | 0.61        | 0.0026  |
| 4217                     | 0.63                            | 0.85                 | 5.1               | 2.76                          | 0.48                | 0.107                | 0.81        | 0.0015  |
| 5623                     | 0.81                            | 0.97                 | 5.95              | 3.07                          | 0.58                | 0.123                | 1.06        | 0.00062 |
| 7499                     | 1.03                            | 1.08                 | 6.9               | 3.43                          | 0.7                 | 0.143                | 1.34        | 0.00048 |
| 10000                    | 1.27                            | 1.17                 | 7.8               | 3.75                          | 0.83                | 0.165                | 1.67        | 0.00028 |

<sup>a</sup> The numbers in parentheses are the threshold energies in eV in the laboratory frame.

We have no information on rotational or vibrational excitation in  $H_3^+ - H_2$  collisions. The buildup of internal energy could be important for the dissociation of drifting  $H_3^+$  in  $H_2$ .

The cross sections for the production of fast H,  $H_2$ ,  $H^+$ , and  $H_2^+$  are from McClure<sup>86</sup> for energies above 4 keV. The cross sections for production of fast  $H^+$  and  $H_2^+$  at energies between 100 and 400 eV are from Lange, Huber, and Wiesmann<sup>94</sup> and are used to extrapolate to threshold as shown by the short-dashed curves. Huber, Schulz, and Wiesmann<sup>95</sup> found a slower increase with energy for the production of slow ions, presumably  $H_2^+$ . The total destruction cross section for  $H_3^+$  in collisions with  $H_2$  (not shown) has been measured by Williams, Geddes, and Gilbody<sup>96</sup> for  $\epsilon_L > 2.5$  keV and is approximately equal to an appropriately weighted sum of the reaction cross sections shown. Further mea-

surements of  $H_3^+ - H_2$  ion-molecule reactions at  $1 \text{ eV} < \epsilon_L < 1 \text{ keV}$  are urgently needed for accurate modeling of low-pressure  $H_2$  discharges.

The Lyman- $\alpha$  excitation cross sections are from Dunn *et al.*,<sup>50</sup> while the Balmer- $\alpha$  cross sections are from Williams *et al.*<sup>46</sup> These data are extrapolated to their respective thresholds, as shown. The data of Williams *et al.*<sup>46</sup> show that the fraction of the H $\alpha$  emitted by fast H atoms increases from  $\sim 0.5$  at 3 keV to 0.7 at 10 keV.

The cross section for electron production  $e$  is from Barnett *et al.*<sup>15</sup> and is extrapolated to threshold as shown.

## 5.2. Drift Velocity and Destruction of $H_3^+$ in $H_2$

Calculated and measured drift velocities of  $H_3^+$  in  $H_2$  are compared in Fig. 7 and the calculated values are tabulat-

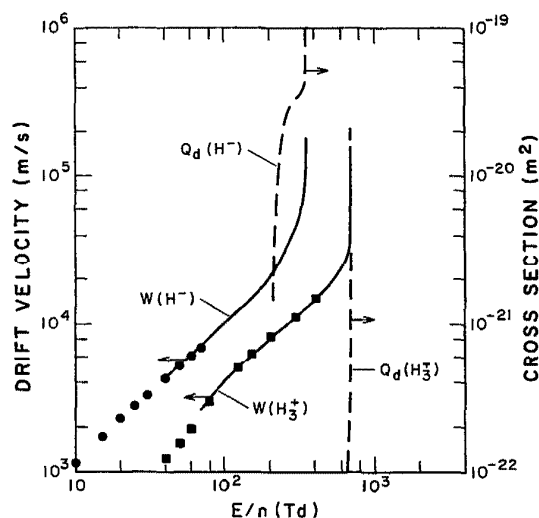


FIG. 7. Drift velocities  $W(H_3^+)$  and  $W(H^-)$  and destruction cross sections  $Q_d(H_3^+)$  and  $Q_d(H^-)$  in  $H_2$  versus  $E/n$ . The curves were calculated using the momentum balance model of Eq. (4). The square points are experimental drift velocities for  $H_3^+$  from Miller *et al.*,<sup>66</sup> while the circles are for  $H^-$  from Graham *et al.*<sup>125</sup> The calculated results are listed in Table 7.

ed in Table 7. As for  $H^+$ , the  $Q_m$  values for  $H_3^+$  in  $H_2$  are adjusted until the drift velocities calculated using the single-beam, momentum-balance model of Sec. 3.3 agree with experiment.<sup>66</sup> Note that at the  $H_3^+$  energies of these calculations only the recoil term of Eq. (3) contributes to  $L_m(\epsilon_L)$ .  $H_3^+$  runaway occurs for  $E/n > 700$  Td. Also shown are the cross sections for  $H_3^+$  destruction at the energies of the ion

“beam.” The very rapid rise in the destruction cross section for  $E/n > 600$  Td is consistent with the upper limit to the  $E/n$  at which drift velocity measurements were made.<sup>66</sup> However, one must keep in mind that our single-beam model of Sec. 3.3 has no high-energy “tail” and so may severely underestimate the dissociation coefficient at  $E/n < 700$  Td. The cross section for electron production, i.e., ionization, is negligibly small in the  $E/n$  range for which these steady-state calculations apply. Ionization by  $H_3^+$  is significantly larger than for  $H^+$  for the higher ion energies attained when runaway occurs at  $E/n > 700$  Td.

## 6. H Collisions with $H_2$

### 6.1. H- $H_2$ Cross Sections

The cross sections for momentum transfer in collisions of H with  $H_2$ , shown in Fig. 8 and Table 8 for energies of 500, 1500, and 5000 eV, are calculated from the differential scattering cross sections of Newman *et al.*<sup>28</sup> At energies near 0.1 eV we show the momentum transfer cross sections calculated from the diffusion measurements of Lynch and Michael.<sup>97</sup> The long-dashed lines are calculated from the diffusion coefficient assuming either a constant cross section or a cross section inversely proportional to velocity. Our best estimate is shown by the solid curve and passes through the intersection of the dashed lines. The short-dashed curve is an interpolation between the low- and high-energy data sets and is our present recommendation. We note that at energies below 2 eV, the  $Q_m$  values for H in  $H_2$  are significantly below those for  $H^+$  in  $H_2$ , presumably because of the long-range polarization interaction for the ion. At higher energies, the H in  $H_2$  cross section is larger, because of the larger effective size of the H atom compared to that of  $H^+$ . Note that for energies above 500 eV, the large-angle scattering and  $Q_m$  of

Table 7. Drift velocities and destruction coefficients for  $H_3^+$  and  $H^-$  in  $H_2$ .

| $E/n$<br>(Td) <sup>a</sup> | $H_3^+$ in $H_2$     |                |  | $H^-$ in $H_2$       |                |  |
|----------------------------|----------------------|----------------|--|----------------------|----------------|--|
|                            | $\epsilon_m$<br>(eV) | $W_m$<br>(m/s) | $\alpha_d/n$<br>( $10^{-20} \text{ m}^2$ ) | $\epsilon_m$<br>(eV) | $W_m$<br>(m/s) | $\alpha_d/n$<br>( $10^{-20} \text{ m}^2$ ) |
| 50                         | <0.1                 |                |  | 0.15                 | 5380           |  |
| 100                        | 0.25                 | 4010           |  | 0.53                 | 10100          |  |
| 150                        | 0.56                 | 6000           |  | 1.13                 | 14770          |  |
| 200                        | 1                    | 8020           |  | 2.1                  | 20100          | <0.01                                      |
| 250                        | 1.34                 | 9280           |  | 4.9                  | 30800          | 2.1  |
| 300                        | 1.95                 | 11200          |  | 10.2                 | 44400          | 3.4  |
| 330                        | 2.28                 | 12110          |  | 17                   | 57300          | 3.9  |
| 360                        | 2.73                 | 13250          |  | runaway              |                | >5.0                                       |
| 400                        | 3.21                 | 14370          |  |                      |                |  |
| 500                        | 5.1                  | 18110          |  |                      |                |  |
| 600                        | 8.8                  | 23800          |  |                      |                |  |
| 650                        | 11.6                 | 27300          | <0.001                                     |                      |                |  |
| 670                        | 13.2                 | 29100          | 0.015                                      |                      |                |  |
| 690                        | 18                   | 34000          | 0.095                                      |                      |                |  |
| 699                        | 24                   | 39300          | 0.16                                       |                      |                |  |
| 700                        | runaway              |                | >0.5                                       |                      |                |  |

<sup>a</sup> 1 Td =  $10^{-21}$  v  $\text{m}^2$

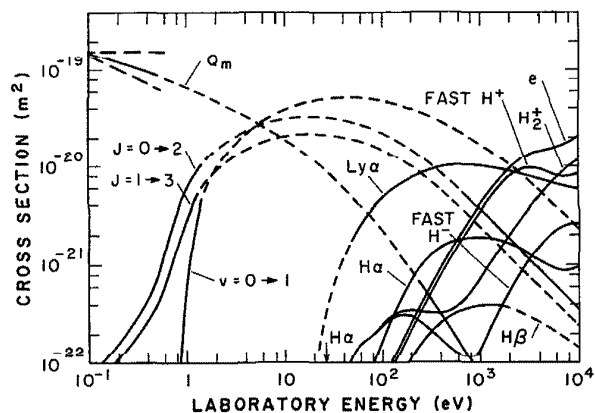


FIG. 8. Cross sections for collisions of H with  $H_2$  versus laboratory energy of H, for  $H_2$  at rest. The solid curves are based on experiment or theory while the short-dashed curves are extrapolations or interpolations. The curves show cross sections for momentum transfer  $Q_m$ ; rotational excitation for  $J = 0 \rightarrow 2$  and  $J = 1 \rightarrow 3$ ; vibrational excitation for  $v = 0 \rightarrow 1$ ; ionization and ion-pair formation resulting in  $H_2^+$ , fast  $H^+$  and/or  $H^-$ ; Ly- $\alpha$ , H $\alpha$  and H $\beta$  excitation; and electron production ( $e$ ). The arrow indicates the threshold energy for H $\alpha$  excitation. These cross sections are listed in Table 8.

H by  $H_2$  approaches<sup>28</sup> that for Coulomb collisions of  $H^+$  with the  $H^+$  nuclei of the  $H_2$ .

The cross sections for the rotational excitation of  $H_2$  by H shown in Fig. 8 for  $\epsilon_L < 3.7$  eV are smoothed values from theory by Green and Truhlar<sup>98</sup> and are somewhat larger than the larger of the theoretical results of McCann and Flannery.<sup>99</sup> The adopted cross sections are in good agreement with the very recent experimental data of Levene *et al.*<sup>100</sup> at 1.7 eV. For  $\epsilon_L > 3.7$  eV we adopt the  $(\epsilon_L)^{-1}$  dependence and magnitude, calculated theoretically by Ioup and Russek<sup>101</sup> for  $\epsilon_L > 750$  eV. Note that the cross sections for rotational excitation of  $H_2$  by H rise much more slowly above threshold than the corresponding values for  $H^+$ , probably due to the absence of the charge-quadrupole interaction for H- $H_2$ .

An average cross section for vibrational deexcitation of  $H_2(v = 1)$  by H of about  $10^{-22} m^{-2}$  at 300 K, were found by Heidner and Kasper.<sup>102</sup> This value is considerably larger than those given by several theoretical cross sections at such low energies.<sup>103</sup> Recent measurements of cross sections for vibrational excitation for  $v'' = 0, J'' = 0$  to  $v' = 1, J' = 1$  or 3, by Nieh and Valentini,<sup>104</sup> at  $1.02 < \epsilon_L < 1.65$  eV, show resonant structure, superimposed on a background cross section of  $\approx 2 \times 10^{-22} m^{-2}$ . The theoretical excitation cross sections calculated from deexcitation cross sections (all  $\Delta J$ ) from Jansen op de Haar and Balint-Kurti<sup>105</sup> are much larger and increase rapidly with energy in this  $\epsilon_L$  range. The theoretical excitation cross sections of Zhang and Miller<sup>106</sup> for  $v = 0-1$  and  $J = 0-1$  or 3, agree with experiment in overall magnitude but not with regard to the structure. On the basis of presently available information, Russek<sup>59</sup> does not expect the potential energy surface of Ioup and Russek<sup>101</sup> to yield reliable vibrational-excitation cross sections. Until these

problems are resolved, we recommend in Fig. 8 the theoretically based vibrational excitation cross sections of Schatz<sup>103</sup> at low energies and the estimated curve based on the  $H^+ + H_2$  cross sections for high energies.

For energies between 80 and 1000 eV we use the Balmer- $\alpha$  and - $\beta$  data (labeled H $\alpha$  and H $\beta$ ) of Van Zyl *et al.*,<sup>107</sup> while for higher energies we show the Balmer- $\alpha$  results of Williams *et al.*<sup>46</sup> The experiments of Williams *et al.* show that most of the H $\alpha$  excitation results in fast, excited H atoms, especially at the lower energies. The Lyman- $\alpha$  curve of Fig. 8 for energies above 150 eV is from Birely and McNeal,<sup>108</sup> while that for lower energies is from the very recent results of Van Zyl, Gealy, and Neumann.<sup>109</sup> The only data found for excitation of  $H_2$  molecular emission were for 50 keV, for which the estimated-excitation cross section<sup>49</sup> for the Lyman bands was  $\approx 1.6 \times 10^{-21} m^2$ .

The cross sections for electron production in Fig. 8 and Table 8 are taken to be equal to the sum of the cross sections for  $e + H^+$  and  $e + H_2^+$  production, measured by Van Zyl, Le, and Amme.<sup>110</sup>

The cross sections for the production of  $H_2^+$ , fast  $H^+$ , and fast  $H^-$  in Fig. 8 are also taken from Van Zyl, Le, and Amme.<sup>110</sup>

## 6.2. Stopping Power for H in $H_2$

The contributions of vibrational excitation, electronic excitation and ionization to the stopping power  $L_e$  for fast H in  $H_2$ , calculated using our cross-section set and Eq. (1), are shown by the dashed curves in Fig. 9 and listed in Table 9. The contribution of rotational excitation is too small to show, although it may be significantly underestimated because of our neglect of large changes in the rotational quantum number<sup>59</sup> at large  $\epsilon_L$ . Two estimates of the total stopping power for inelastic energy loss and for ionization are shown. The lower curve shown for the loss function due to ionization is calculated using the cross section for ionization shown in Fig. 8 and the energy loss to electrons found for  $H^+ - H_2$  collisions, and given by Eq. (2). The lower solid curve is the total inelastic loss function or inelastic stopping power, obtained by adding the lower ionization curve to the loss functions for vibrational and electronic excitation. This calculation is  $\sim 20\%$  lower than the stopping power determined from measurements<sup>63</sup> of the energy of the  $H^+$  in a beam with an equilibrium H- $H^+$  composition passing through  $H_2$  (shown in Fig. 9, by the points). Loss of energy in momentum-transfer or recoil collisions is omitted from  $L_e$  for this comparison, since  $H^+$  ions formed from H atoms undergoing large-angle scattering are not analyzed by the detector.

A second estimate of the energy-loss function caused by ionization is obtained by assuming that the energy loss is the same as the average energy loss measured for electrons by Opal, Peterson, and Beaty.<sup>111</sup> This approximation leads to the upper curves for the ionization and total loss functions. In this case, the calculated stopping power  $L_e$  is  $\sim 50\%$  larger than the measured values.<sup>63</sup> We conclude that the agreement of experiment and the calculations are well within our

Table 8. Cross sections for H + H<sub>2</sub> collisions tabulated by product(s).  
(Cross sections in units of 10<sup>-20</sup> m<sup>2</sup>)

| Lab.<br>Energy<br>eV | Product                       |                 |                 |                               |                                  |                     | Ly α<br>(22.5) | Hα<br>(24) | Hβ<br>(25.5) | e<br>(23.1) | Q <sub>m</sub> |
|----------------------|-------------------------------|-----------------|-----------------|-------------------------------|----------------------------------|---------------------|----------------|------------|--------------|-------------|----------------|
|                      | J=0-2<br>(0.066) <sup>a</sup> | J=1-3<br>(0.11) | v=0-1<br>(0.81) | fast H <sup>-</sup><br>(22.5) | slow H <sub>2</sub> <sup>+</sup> | fast H <sup>+</sup> |                |            |              |             |                |
| 0.100                | 0.0067                        | 0.0048          |                 |                               |                                  |                     |                |            |              |             | 15.1           |
| 0.133                | 0.0095                        | 0.0067          |                 |                               |                                  |                     |                |            |              |             | 13.8           |
| 0.178                | 0.014                         | 0.0098          |                 |                               |                                  |                     |                |            |              |             | 12.7           |
| 0.237                | 0.0203                        | 0.014           |                 |                               |                                  |                     |                |            |              |             | 11.5           |
| 0.316                | 0.031                         | 0.0197          |                 |                               |                                  |                     |                |            |              |             | 10.3           |
| 0.422                | 0.052                         | 0.03            |                 |                               |                                  |                     |                |            |              |             | 9.4            |
| 0.562                | 0.117                         | 0.056           |                 |                               |                                  |                     |                |            |              |             | 8.3            |
| 0.750                | 0.305                         | 0.135           |                 |                               |                                  |                     |                |            |              |             | 7.4            |
| 1.000                | 0.59                          | 0.305           | 0.076           |                               |                                  |                     |                |            |              |             | 6.6            |
| 1.334                | 0.97                          | 0.56            | 0.365           |                               |                                  |                     |                |            |              |             | 5.9            |
| 1.778                | 1.35                          | 0.8             | 0.77            |                               |                                  |                     |                |            |              |             | 5.1            |
| 2.371                | 1.73                          | 1.06            | 1.23            |                               |                                  |                     |                |            |              |             | 4.4            |
| 3.162                | 2.07                          | 1.3             | 1.7             |                               |                                  |                     |                |            |              |             | 3.75           |
| 4.217                | 2.4                           | 1.54            | 2.23            |                               |                                  |                     |                |            |              |             | 3.2            |
| 5.623                | 2.69                          | 1.76            | 2.8             |                               |                                  |                     |                |            |              |             | 2.7            |
| 7.499                | 2.93                          | 1.93            | 3.35            |                               |                                  |                     |                |            |              |             | 2.26           |
| 10.00                | 3.11                          | 2.07            | 3.85            |                               |                                  |                     |                |            |              |             | 1.87           |
| 13.34                | 3.2                           | 2.14            | 4.3             |                               |                                  |                     |                |            |              |             | 1.56           |
| 17.78                | 3.24                          | 2.18            | 4.7             |                               |                                  |                     |                |            |              |             | 1.23           |
| 23.71                | 3.24                          | 2.18            | 4.95            | 0.0002                        | 0.0002                           |                     | 0.022          |            |              |             | 0.98           |
| 31.62                | 3.13                          | 2.12            | 5.13            | 0.0033                        | 0.0033                           |                     | 0.064          | 0.00018    |              |             | 0.77           |
| 42.17                | 2.97                          | 2.03            | 5.23            | 0.009                         | 0.009                            |                     | 0.138          | 0.0007     |              | 0.00027     | 0.58           |
| 56.23                | 2.77                          | 1.87            | 5.2             | 0.0148                        | 0.0148                           | 0.0015              | 0.237          | 0.003      |              | 0.00107     | 0.43           |
| 74.99                | 2.5                           | 1.71            | 5.05            | 0.0186                        | 0.0186                           | 0.0024              | 0.355          | 0.0082     |              | 0.003       | 0.305          |
| 100.0                | 2.22                          | 1.51            | 4.75            | 0.024                         | 0.0255                           | 0.0053              | 0.49           | 0.0175     | 0.0028       | 0.0064      | 0.214          |
| 133.4                | 1.93                          | 1.3             | 4.47            | 0.03                          | 0.032                            | 0.01                | 0.6            | 0.035      | 0.0053       | 0.012       | 0.15           |
| 177.8                | 1.64                          | 1.11            | 4.08            | 0.0313                        | 0.034                            | 0.0185              | 0.72           | 0.058      | 0.0093       | 0.022       | 0.103          |
| 237.1                | 1.34                          | 0.89            | 3.65            | 0.027                         | 0.033                            | 0.032               | 0.83           | 0.091      | 0.015        | 0.038       | 0.067          |
| 316.2                | 1.07                          | 0.71            | 3.25            | 0.0215                        | 0.0327                           | 0.054               | 0.92           | 0.128      | 0.021        | 0.064       | 0.045          |
| 421.7                | 0.84                          | 0.55            | 2.84            | 0.0166                        | 0.0328                           | 0.089               | 0.99           | 0.156      | 0.0272       | 0.105       | 0.029          |
| 562.3                | 0.64                          | 0.41            | 2.45            | 0.0129                        | 0.0373                           | 0.146               | 1.03           | 0.176      | 0.0323       | 0.17        | 0.0185         |
| 749.9                | 0.475                         | 0.305           | 2.05            | 0.0116                        | 0.05                             | 0.235               | 1.04           | 0.184      | 0.0364       | 0.27        | 0.0117         |
| 1000.                | 0.36                          | 0.23            | 1.7             | 0.014                         | 0.0745                           | 0.355               | 1.02           | 0.187      | 0.039        | 0.41        | 0.0075         |
| 1334.                | 0.272                         | 0.169           | 1.4             | 0.0247                        | 0.113                            | 0.515               | 0.98           | 0.182      | 0.0397       | 0.59        | 0.0048         |
| 1778.                | 0.202                         | 0.132           | 1.12            | 0.044                         | 0.173                            | 0.71                | 0.93           | 0.169      | 0.0383       | 0.82        | 0.003          |
| 2371.                | 0.15                          | 0.101           | 0.89            | 0.073                         | 0.258                            | 0.89                | 0.86           | 0.15       | 0.0347       | 1.09        | 0.002          |
| 3162.                | 0.113                         | 0.075           | 0.71            | 0.113                         | 0.37                             | 0.96                | 0.79           | 0.128      | 0.03         | 1.33        | 0.0013         |
| 4217.                | 0.085                         | 0.057           | 0.53            | 0.16                          | 0.53                             | 0.92                | 0.73           | 0.108      | 0.0255       | 1.47        | 0.00078        |
| 5623.                | 0.064                         | 0.043           | 0.4             | 0.213                         | 0.71                             | 0.82                | 0.67           | 0.093      | 0.0216       | 1.56        | 0.0005         |
| 7499.                | 0.0475                        | 0.032           | 0.297           | 0.25                          | 0.95                             | 0.78                | 0.63           | 0.089      | 0.0177       | 1.74        | 0.00032        |
| 10000.               | 0.036                         | 0.024           | 0.225           | 0.256                         | 1.17                             | 0.84                | 0.6            | 0.098      | 0.0147       | 2.03        | 0.00019        |

<sup>a</sup> The numbers in parentheses are the nominal thresholds in the laboratory frame in eV.

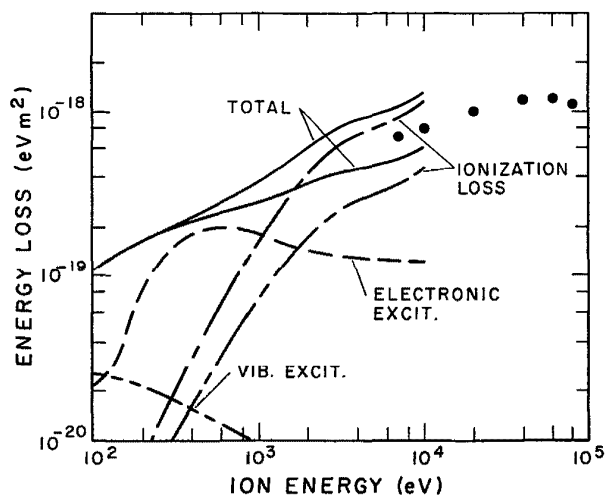


FIG. 9. Energy loss  $L_e$  coefficients for H in  $H_2$  versus H laboratory energy. The solid curves show the inelastic portion of the total loss coefficients defined by Eq. (1) from 0.1 to 100 keV. The chain curves show the two estimates of the energy loss due to ionization, while the two solid curves show the corresponding total energy loss calculations. The dashed curves show the contributions resulting from vibrational excitation and electronic excitation. The points show the experimental results of Phillips.<sup>63</sup> The larger set of energy loss coefficients for H in  $H_2$  are listed in Table 9.

Table 9. Energy loss function for H in  $H_2$ . (Energy loss in  $10^{-20}$  eV  $m^2$ )

| Lab. energy<br>eV | Process   |        |        |         |         |          |         |
|-------------------|-----------|--------|--------|---------|---------|----------|---------|
|                   | L(recoil) | L(rot) | L(vib) | L(elec) | L(ion)  | L(inela) | L(tot)  |
| 0.100             | 0.671     |        |        |         |         |          | 0.671   |
| 0.133             | 0.818     |        |        |         |         |          | 0.818   |
| 0.178             | 1.004     |        |        |         |         |          | 1.004   |
| 0.237             | 1.212     |        |        |         |         |          | 1.213   |
| 0.316             | 1.448     | 0.001  |        |         |         | 0.001    | 1.449   |
| 0.422             | 1.762     | 0.002  |        |         |         | 0.002    | 1.764   |
| 0.562             | 2.074     | 0.004  |        |         |         | 0.004    | 2.079   |
| 0.750             | 2.466     | 0.011  |        |         |         | 0.011    | 2.477   |
| 1.000             | 2.933     | 0.023  | 0.041  |         |         | 0.064    | 2.998   |
| 1.334             | 3.497     | 0.041  | 0.197  |         |         | 0.238    | 3.735   |
| 1.778             | 4.031     | 0.059  | 0.416  |         |         | 0.474    | 4.505   |
| 2.371             | 4.637     | 0.077  | 0.664  |         |         | 0.741    | 5.379   |
| 3.162             | 5.270     | 0.094  | 0.918  |         |         | 1.012    | 6.282   |
| 4.217             | 5.997     | 0.111  | 1.204  |         |         | 1.315    | 7.312   |
| 5.623             | 6.748     | 0.126  | 1.512  |         |         | 1.638    | 8.386   |
| 7.499             | 7.532     | 0.138  | 1.809  |         |         | 1.947    | 9.479   |
| 10.000            | 8.311     | 0.148  | 2.079  |         |         | 2.227    | 10.538  |
| 13.335            | 9.246     | 0.152  | 2.322  |         |         | 2.474    | 11.720  |
| 17.783            | 9.721     | 0.155  | 2.538  |         |         | 2.693    | 12.414  |
| 23.714            | 10.329    | 0.155  | 2.673  | 0.333   |         | 3.161    | 13.490  |
| 31.623            | 10.822    | 0.151  | 2.770  | 1.012   |         | 3.933    | 14.755  |
| 42.170            | 10.870    | 0.144  | 2.824  | 2.216   | 0.005   | 5.189    | 16.060  |
| 56.234            | 10.747    | 0.133  | 2.808  | 3.825   | 0.022   | 6.788    | 17.534  |
| 74.989            | 10.165    | 0.121  | 2.727  | 5.735   | 0.066   | 8.650    | 18.815  |
| 100.000           | 9.511     | 0.107  | 2.565  | 8.112   | 0.153   | 10.937   | 20.448  |
| 133.352           | 8.890     | 0.092  | 2.414  | 10.241  | 0.311   | 13.058   | 21.948  |
| 177.828           | 8.141     | 0.079  | 2.203  | 12.618  | 0.613   | 15.513   | 23.654  |
| 237.137           | 7.061     | 0.063  | 1.971  | 14.964  | 1.135   | 18.133   | 25.194  |
| 316.228           | 6.325     | 0.051  | 1.755  | 17.084  | 2.040   | 20.930   | 27.255  |
| 421.697           | 5.435     | 0.039  | 1.534  | 18.779  | 3.562   | 23.914   | 29.349  |
| 562.341           | 4.624     | 0.029  | 1.323  | 19.865  | 6.117   | 27.334   | 31.958  |
| 749.894           | 3.899     | 0.022  | 1.107  | 20.302  | 10.274  | 31.705   | 35.604  |
| 1000.000          | 3.333     | 0.017  | 0.918  | 20.199  | 16.454  | 37.588   | 40.921  |
| 1333.521          | 2.845     | 0.012  | 0.756  | 19.710  | 24.909  | 45.387   | 48.232  |
| 1778.279          | 2.371     | 0.009  | 0.605  | 18.981  | 36.334  | 55.929   | 58.300  |
| 2371.374          | 2.108     | 0.007  | 0.481  | 17.905  | 50.582  | 68.487   | 68.975  |
| 3162.278          | 1.827     | 0.005  | 0.383  | 16.899  | 64.510  | 81.797   | 83.624  |
| 4216.965          | 1.462     | 0.004  | 0.286  | 16.188  | 74.389  | 90.866   | 92.328  |
| 5623.413          | 1.250     | 0.003  | 0.216  | 15.673  | 82.222  | 98.114   | 99.364  |
| 7498.942          | 1.067     | 0.002  | 0.160  | 15.394  | 95.370  | 110.927  | 111.993 |
| 10000.00          | 0.844     | 0.002  | 0.122  | 15.048  | 115.537 | 130.708  | 131.552 |

knowledge of the energy losses in the ionization processes and that the average of our two estimates gives a satisfactory fit to experiment.<sup>63</sup> We have not found any theoretical predictions for the stopping power for H in H<sub>2</sub> at  $\epsilon_L < 10$  keV.

## 7. H<sub>2</sub> Collisions with H<sub>2</sub>

### 7.1. H<sub>2</sub>-H<sub>2</sub> Cross Sections

The only information we have on large-angle scattering in low-energy H<sub>2</sub>-H<sub>2</sub> collisions is from experimental viscosity data at temperatures up to 1100 K. We show in Fig. 10 and Table 10 the momentum-transfer cross sections calculated from the viscosity data, assuming isotropic scattering.<sup>113</sup> At energies above 1 keV, we suggest the use of momentum-transfer cross sections scaled upward by a factor of 1.8, according to the mass dependence of screened Coulomb theory<sup>56</sup> from the cross sections for H<sup>+</sup> in H<sub>2</sub> shown in Fig. 1. Our interpolation between low and high energies, as shown by the short-dashed curve in Fig. 10 and the recommended cross sections, is given in Table 10.

Rate coefficients for rotational relaxation of H<sub>2</sub> by H<sub>2</sub> have been measured up to 1200 K.<sup>114</sup> Cross sections for rotational excitation have been calculated<sup>115</sup> for energies up to ~4 eV, as shown in Fig. 10. Since we have no cross sections for higher energies, we have assumed the cross sections to decrease roughly as the mean of the curves for H<sup>+</sup>-H<sub>2</sub> collisions (Fig. 1) and for H-H<sub>2</sub> (Fig. 8).

The rate coefficients for vibrational deexcitation of H<sub>2</sub> by H<sub>2</sub> have been measured<sup>116,117</sup> at temperatures from 40 to 3000 K and are found to increase rapidly with increasing temperature at > 200 K. When converted to vibrational-excitation cross sections, these results extrapolate well to the

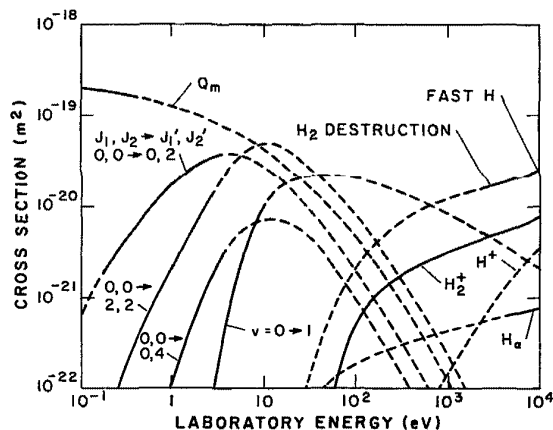


FIG. 10. Cross sections for collisions of H<sub>2</sub> with H<sub>2</sub> versus laboratory energy of the projectile H<sub>2</sub> for the target H<sub>2</sub> at rest. The solid curves are based on experiment or theory while the short-dashed curves are extrapolations or interpolations. The curves show cross sections for momentum transfer  $Q_m$ ; rotational excitation for  $J_1, J_2 = 0,0 \rightarrow 0,2$ ,  $0,0 \rightarrow 2,2$ , and  $0,0 \rightarrow 0,4$ ; vibrational excitation for  $v = 0 \rightarrow 1$ ; fast H<sub>2</sub> destruction and fast H formation; ionization to form H<sub>2</sub><sup>+</sup> and H<sup>+</sup>; and H $\alpha$  excitation. These cross sections are listed in Table 10.

higher energy theoretical calculations of Gianturco and Lamanna,<sup>118</sup> shown in Fig. 10 for  $\epsilon_L < 5$  eV. We have extrapolated these data to 10 keV using the cross sections for vibrational excitation in H<sub>2</sub><sup>+</sup>-H<sub>2</sub> collisions shown in Fig. 4, i.e., we assume that the nuclear charges dominate the H<sub>2</sub>-H<sub>2</sub> interaction at the highest energies.

The cross sections for excitation of the Balmer- $\alpha$  line in H<sub>2</sub>-H<sub>2</sub> collisions have been measured for  $\epsilon_L \geq 10$  keV.<sup>119</sup> Since some kind of estimate for such data is essential for analyses of our electrical discharges at very high  $E/n$ , we have extrapolated the results of Williams *et al.*<sup>119</sup> to lower energies, as shown in Fig. 10. We have found no data on the excitation of Lyman- $\alpha$  or of H<sub>2</sub> bands or continuum by fast H<sub>2</sub>.<sup>49</sup> This is unfortunate, since experiments in deuterium<sup>120</sup> and hydrogen<sup>121</sup> suggest the possible importance of such excitation processes.

We have adopted the low-energy cross sections for H<sub>2</sub><sup>+</sup> formation and ionization from Peterson and Eisner,<sup>122</sup> rather than the values of Noda,<sup>123</sup> because of the larger ion-collection angle used by Peterson and Eisner. At  $\epsilon_L > 5$  keV, our curve approaches that of McClure.<sup>124</sup> McClure's cross sections for fast H and H<sup>+</sup> formation have been rather arbitrarily extrapolated to lower energies in order to provide estimates for discharge modeling.

### 7.2. H<sub>2</sub>-H<sub>2</sub> Average Cross Sections

When fast H<sub>2</sub> molecules are formed in charge-transfer collisions between H<sub>2</sub><sup>+</sup> and cold H<sub>2</sub>, the fast H<sub>2</sub> molecules are assumed to have the same velocity distribution as the H<sub>2</sub><sup>+</sup>. It is therefore desirable to have available the cross sections for fast H<sub>2</sub>-H<sub>2</sub> collisions averaged over the equilibrium energy distributions for the H<sub>2</sub><sup>+</sup>. Figure 11 and Table 11 give the average cross sections for the ionization and excitation processes of Fig. 10 as calculated using Eq. (10). Also shown is the average cross section for the sum of momentum-transfer (large-angle scattering) and inelastic collisions. In some models, e.g., that of Phelps and Jelenković for Ar,<sup>10</sup> such collisions are assumed to effectively destroy the fast neutral beam because they result in sufficient energy loss to reduce the energy below that for which there is significant excitation or ionization. Note that at 10 kTd the calculated "second Townsend" or spatial-ionization coefficients for fast H<sub>2</sub> in H<sub>2</sub> are about five times those shown in Fig. 5 for H<sub>2</sub><sup>+</sup> in H<sub>2</sub> with the same energy distribution. This ratio, along with the efficient production of fast H<sub>2</sub>, means that in high  $E/n$  discharges, ionization of H<sub>2</sub> by fast H<sub>2</sub> will often be much more important than ionization by equally fast H<sub>2</sub><sup>+</sup>.

## 8. H<sup>-</sup> Collisions with H<sub>2</sub>

The values of  $Q_m(\epsilon_L)$ , shown in Fig. 12 and Table 12, for energies below 1 eV were obtained by adjusting the  $Q_m$  values to obtain a fit between the measured H<sup>-</sup> drift velocities<sup>125</sup> shown in Fig. 7 and those calculated and listed in Table 7 using the single-beam, momentum-balance model discussed in Sec. 3.3. The resultant cross sections are consis-

Table 10. Cross sections for  $H_2 + H_2$  collisions tabulated by product(s).  
(Cross sections in units of  $10^{-20} m^2$ )

| Lab. ion<br>energy<br>eV | $H_2$ dest. | Product                      |                  |                  |                 |                   | $H^+ + H$<br>39.6 | $H\alpha$<br>32 | Ioniz.<br>30.8 | $Q_m$    |
|--------------------------|-------------|------------------------------|------------------|------------------|-----------------|-------------------|-------------------|-----------------|----------------|----------|
|                          |             | $H_2^+$<br>30.4 <sup>a</sup> | J,J=0,2<br>0.088 | J,J=2,2<br>0.176 | J,J=0,4<br>0.29 | $v = 0-1$<br>1.04 |                   |                 |                |          |
| 0.1                      |             |                              | 0.063            |                  |                 |                   |                   |                 | 19.8           |          |
| 0.1334                   |             |                              | 0.12             |                  |                 |                   |                   |                 | 18.9           |          |
| 0.1776                   |             |                              | 0.186            |                  |                 |                   |                   |                 | 16.2           |          |
| 0.237                    |             |                              | 0.30             | 0.009            |                 |                   |                   |                 | 17.4           |          |
| 0.316                    |             |                              | 0.45             | 0.0197           |                 |                   |                   |                 | 16.6           |          |
| 0.422                    |             |                              | 0.655            | 0.039            |                 |                   |                   |                 | 15.6           |          |
| 0.562                    |             |                              | 0.82             | 0.069            |                 |                   |                   |                 | 14.7           |          |
| 0.750                    |             |                              | 1.27             | 0.12             | 0.0051          |                   |                   |                 | 13.6           |          |
| 1                        |             |                              | 1.7              | 0.214            | 0.0124          |                   |                   |                 | 12.5           |          |
| 1.334                    |             |                              | 2.17             | 0.365            | 0.0285          |                   |                   |                 | 11.4           |          |
| 1.778                    |             |                              | 2.68             | 0.64             | 0.065           |                   |                   |                 | 10.35          |          |
| 2.371                    |             |                              | 3.2              | 1.06             | 0.13            | 0.004             |                   |                 | 9.43           |          |
| 3.162                    |             |                              | 3.63             | 1.74             | 0.24            | 0.019             |                   |                 | 8.25           |          |
| 4.217                    |             |                              | 3.75             | 2.63             | 0.39            | 0.082             |                   |                 | 7.15           |          |
| 5.623                    |             |                              | 3.6              | 3.65             | 0.53            | 0.245             |                   |                 | 6.15           |          |
| 7.50                     |             |                              | 3.25             | 4.47             | 0.64            | 0.55              |                   |                 | 5.15           |          |
| 10                       |             |                              | 2.76             | 4.9              | 0.71            | 1.07              |                   |                 | 4.25           |          |
| 13.34                    |             |                              | 2.22             | 4.75             | 0.71            | 1.52              |                   |                 | 3.43           |          |
| 17.78                    | 0.0006      |                              | 1.68             | 4.15             | 0.65            | 1.82              | 0.0009            |                 | 2.68           |          |
| 23.7                     | 0.0033      |                              | 1.23             | 3.38             | 0.57            | 2.04              | 0.003             |                 | 2.1            |          |
| 31.6                     | 0.0144      |                              | 0.89             | 2.66             | 0.455           | 2.15              | 0.0058            |                 | 1.59           |          |
| 42.1                     | 0.036       | 0.0009                       | 0.625            | 2.02             | 0.335           | 2.21              | 0.0085            | 0.0009          | 1.19           |          |
| 56.2                     | 0.075       | 0.0065                       | 0.435            | 1.48             | 0.225           | 2.20              | 0.0125            | 0.0065          | 0.87           |          |
| 75.0                     | 0.134       | 0.0255                       | 0.295            | 1.06             | 0.148           | 2.15              | 0.0155            | 0.0255          | 0.63           |          |
| 100                      | 0.215       | 0.0515                       | 0.197            | 0.765            | 0.095           | 2.04              | 0.0185            | 0.0515          | 0.445          |          |
| 133.4                    | 0.31        | 0.082                        | 0.128            | 0.54             | 0.059           | 1.90              | 0.0214            | 0.082           | 0.315          |          |
| 177.8                    | 0.425       | 0.113                        | 0.082            | 0.363            | 0.037           | 1.74              | 0.00075           | 0.0247          | 0.11375        | 0.212    |
| 237                      | 0.57        | 0.149                        | 0.051            | 0.24             | 0.0225          | 1.57              | 0.0013            | 0.0278          | 0.1443         | 0.136    |
| 316                      | 0.705       | 0.175                        | 0.0315           | 0.157            | 0.0137          | 1.40              | 0.0021            | 0.0308          | 0.1771         | 0.088    |
| 422                      | 0.83        | 0.21                         | 0.0193           | 0.102            | 0.0085          | 1.25              | 0.0034            | 0.0343          | 0.2134         | 0.055    |
| 562                      | 0.97        | 0.247                        | 0.0115           | 0.063            |                 | 1.11              | 0.0055            | 0.0373          | 0.2525         | 0.034    |
| 750                      | 1.11        | 0.284                        | 0.009            | 0.037            |                 | 0.96              | 0.009             | 0.0405          | 0.293          | 0.0202   |
| 1000                     | 1.23        | 0.323                        |                  | 0.0217           |                 | 0.825             | 0.0153            | 0.0443          | 0.3383         | 0.0114   |
| 1334                     | 1.36        | 0.363                        |                  | 0.0128           |                 | 0.715             | 0.0243            | 0.048           | 0.3873         | 0.0065   |
| 1778                     | 1.48        | 0.405                        |                  | 0.0075           |                 | 0.605             | 0.0385            | 0.0517          | 0.4435         | 0.0034   |
| 2371                     | 1.60        | 0.445                        |                  |                  |                 | 0.515             | 0.060             | 0.056           | 0.505          | 0.0010   |
| 3162                     | 1.71        | 0.487                        |                  |                  |                 | 0.435             | 0.091             | 0.0597          | 0.578          | 0.00103  |
| 4217                     | 1.85        | 0.533                        |                  |                  |                 | 0.36              | 0.135             | 0.0635          | 0.668          | 0.00056  |
| 5623                     | 2.03        | 0.59                         |                  |                  |                 | 0.30              | 0.193             | 0.0675          | 0.783          | 0.0003   |
| 7499                     | 2.24        | 0.665                        |                  |                  |                 | 0.252             | 0.268             | 0.0733          | 0.933          | 0.00016  |
| 10000                    | 2.5         | 0.77                         |                  |                  |                 | 0.212             | 0.37              | 0.0775          | 1.14           | 0.000085 |

<sup>a</sup> Laboratory threshold energy in eV

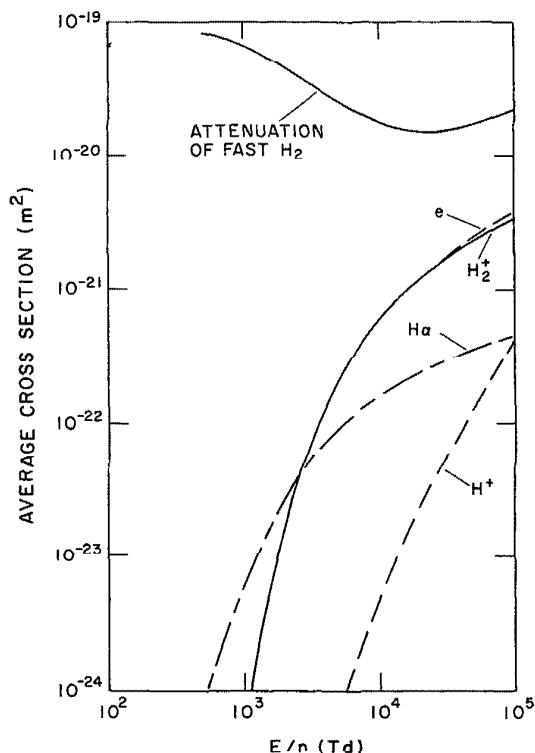


FIG. 11. Average cross sections as a function of  $E/n$  for  $H_2$  formed from  $H_2^+$  drifting through  $H_2$ . The average cross section curves are those for attenuation of the fast  $H_2$  flux; excitation of  $H\alpha$ ; and ionization to produce an electron  $e$  and either  $H_2^+$  or  $H^+$ .

tent with the  $Q_m$  values calculated from 300 K mobility data and extrapolated to higher energies as shown by the long-dashed lines in Fig. 12. Note that the low-energy  $Q_m$  values for  $H^-$  in  $H_2$  are exceptionally small, i.e., about one third those for  $H^+$  in  $H_2$ . At energies above 500 eV, we have assumed that Coulomb scattering dominates at large angles and have used the cross section for  $H^+$  in  $H_2$  from Fig. 1. The interpolation between the low- and high-energy data is shown in Fig. 12.

Table 11. Average cross sections for  $H_2 + H_2$  collisions.

| $E/n$<br>(Td) | $\langle Q(H_2^+) \rangle$<br>(m <sup>2</sup> ) | $\langle Q(H^+) \rangle$<br>(m <sup>2</sup> ) | $\langle Q(H\alpha) \rangle$<br>(m <sup>2</sup> ) | $\langle Q_{ion} \rangle$<br>(m <sup>2</sup> ) | $\langle Q_{att} \rangle$<br>(m <sup>2</sup> ) |
|---------------|---|---|---|--|--|
| 1000          | 5.5E-25 <sup>a</sup>                            | 1.6E-31                                       | 6.0E-24   | 5.5E-25  | 6.6E-20  |
| 2000          | 1.8E-25   | 5.0E-27                                       | 2.9E-23   | 1.8E-23  | 4.5E-20  |
| 3000          | 6.4E-23   | 5.9E-26                                       | 5.2E-23   | 6.4E-23  | 3.5E-20  |
| 5000          | 2.1E-22   | 6.7E-25                                       | 9.2E-23   | 2.1E-22  | 2.5E-20  |
| 10000         | 6.0E-22   | 5.1E-24                                       | 1.6E-22   | 6.0E-22  | 1.8E-20  |
| 20000         | 1.2E-21   | 2.3E-23                                       | 2.4E-22   | 1.2E-21  | 1.5E-20  |
| 30000         | 1.7E-21   | 5.1E-23                                       | 2.8E-22   | 1.7E-21  | 1.5E-20  |
| 50000         | 2.3E-21   | 1.3E-22                                       | 3.5E-22   | 2.4E-21  | 1.7E-20  |
| 100000        | 3.3E-21   | 4.3E-22                                       | 4.5E-22   | 3.7E-21  | 2.1E-20  |

<sup>a</sup>5.5E-25 means  $5.5 \times 10^{-25}$

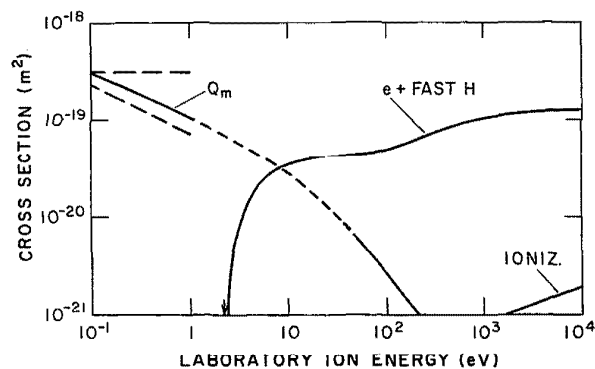


FIG. 12. Cross sections for collisions of  $H^-$  with  $H_2$  versus laboratory energy of  $H^-$  for  $H$ , at rest. The solid curves are based on experiment or theory while the short-dashed curves are extrapolations or interpolations. The curves show cross sections for momentum transfer  $Q_m$ ; detachment to form an electron and fast  $H$  ( $e + \text{FAST } H$ ); and positive ion production (IONIZ.). These cross sections are listed in Table 12. The long-dashed lines are extrapolations to higher energies of fits of constant cross section and constant collision frequency models to 300 K mobility data. The arrow shows the threshold for collisional detachment.

The cross sections in Fig. 12 for electron detachment in  $H^-$  collisions with  $H_2$  are based on the data of Huq, Doverspike, and Champion,<sup>126</sup> at energies from the threshold at 2.18 eV (1.45 eV in center of mass) to about 200 eV, and that of Risley and Geballe<sup>127</sup> for energies from 300 eV to 10 keV.

The cross section for positive ion production<sup>128</sup> is less than 4% of that for detachment at energies below 10 keV, but the  $H^+$  to  $H_2^+$  ratio is unknown.

Cross sections for excitation of  $H$  to very high levels in  $H^-$  collisions with  $H_2$ , have been measured for  $2.3 < \epsilon_L < 60$  keV by Stone and Morgan.<sup>129</sup> One could extrapolate these data to low principal quantum numbers  $n^*$ , and appropriately sum over  $n^*$  to estimate Lyman- $\alpha$ - or Balmer- $\alpha$ -excitation cross sections.

The calculated drift velocity curves for  $H^-$  in  $H_2$  are compared with experimental points<sup>125</sup> in Fig. 7. Also shown are the calculated collisional-detachment cross sections. Detachment increases rapidly for  $E/n > 200$  Td, while runaway does not occur until  $E/n > 350$  Td. Note that these calculations include the detachment term in  $L_m(\epsilon_L)$  for energies above threshold at 2.2 eV or  $E/n > 200$  Td. The validity of this approximation needs to be considered further, since the drift velocity data do not test the model at  $E/n > 70$  Td.

## 9. Discussion

The cross sections compiled in this paper demonstrate the wide range of processes and of experimental and theoretical techniques that need to be considered in order to begin to assemble the "complete" sets needed for modeling. At energies below 10 eV, transport and reaction measurements utilizing swarm, ion cyclotron resonance, and flow-tube techniques, provide much of the available experimental data. At energies above 500 eV, beam scattering techniques yield detailed data such as differential-scattering cross sec-

Table 12. Cross sections for  $H^+ + H_2$  collisions tabulated by product(s)

| Lab. ion<br>energy<br>eV | Detach.<br>10 <sup>-20</sup> m <sup>2</sup> | Q <sub>m</sub><br>10 <sup>-20</sup> m <sup>2</sup> | Detach. &<br>Ionizat.<br>10 <sup>-20</sup> m <sup>2</sup> | L <sub>m</sub><br>10 <sup>-20</sup> eV m <sup>2</sup> |
|--------------------------|---|--|---|---|
| 0.1                      | 0   | 29.4   |   | 3.92  |
| 0.1334                   | 0   | 26.0   |   | 4.62  |
| 0.1778                   | 0   | 23.3   |   | 5.52  |
| 0.237                    | 0   | 20.4   |   | 6.45  |
| 0.316                    | 0   | 18.0   |   | 7.59  |
| 0.421                    | 0   | 15.8   |   | 8.88  |
| 0.562                    | 0   | 13.8   |   | 10.3  |
| 0.750                    | 0   | 12.2   |   | 12.2  |
| 1                        | 0   | 10.55  |   | 14.1  |
| 1.334                    | 0   | 9.20   |   | 16.4  |
| 1.778                    | 0   | 7.90   |   | 18.7  |
| 2.37                     | 0.095                                       | 6.70   |   | 21.2  |
| 3.16                     | 0.78  | 5.75   |   | 24.2  |
| 4.22                     | 1.59  | 4.90   |   | 27.7  |
| 5.62                     | 2.37  | 4.05   |   | 32.2  |
| 7.50                     | 2.96  | 3.37   |   | 38.4  |
| 10                       | 3.42  | 2.75   |   | 44.8  |
| 13.34                    | 3.73  | 2.24   |   | 50.9  |
| 17.78                    | 3.94  | 1.73   |   | 54.5  |
| 23.7                     | 4.1   | 1.33   |   | 57.3  |
| 31.6                     | 4.25  | 1.00   |   | 58.9  |
| 42.2                     | 4.35  | 0.74   |   | 59.4  |
| 56.2                     | 4.43  | 0.54   |   | 59.3  |
| 75.0                     | 4.55  | 0.38   |   | 57.8  |
| 100                      | 4.85  | 0.265  |   | 56.8  |
| 133.4                    | 5.3   | 0.183  |   | 56.6  |
| 177.8                    | 5.9   | 0.123  |   | 57.8  |
| 237                      | 6.6   | 0.081  |   | 60.6  |
| 316                      | 7.35  | 0.053  |   | 65.7  |
| 421                      | 8.2   | 0.034  |   | 73.2  |
| 562                      | 9.0   | 0.021  |   | 81.9  |
| 750                      | 9.7   | 0.0118   |   | 91.3  |
| 1000                     | 10.2  | 0.0072   |   | 101.4   |
| 1334                     | 10.8  | 0.0045   |   | 112.8   |
| 1778                     | 11.3  | 0.0027   | 0.101   | 121.7   |
| 2371                     | 11.8  | 0.00165  | 0.112   | 132.6   |
| 3162                     | 12.1  | 0.001  | 0.124   | 140.9   |
| 4217                     | 12.2  | 0.00062  | 0.139   | 147.4   |
| 5623                     | 12.3  | 0.00038  | 0.154   | 151.7   |
| 7499                     | 12.5  | 0.000235   | 0.172   | 154.8   |
| 10000                    | 12.7  | 0.000145   | 0.19  | 158.1   |

tions. The intermediate energy range is only beginning to be studied. Theory has tended to emphasize energies below about 10 eV, perhaps because of the connection to chemistry, and energies above 10 keV. It is to be hoped that more investigations will be made of the intermediate energy range, including tests of the usefulness of relatively simple theories, such as the Born approximation and simple molecular models.

The cross sections presented in this review provide the basis for modeling of electrical discharges in weakly ionized  $H_2$ . To serve that purpose the cross sections must be "complete." It is hoped that the occasional, somewhat arbitrary, choices and the necessity for estimates of many of the cross sections in critical energy ranges, especially near threshold will encourage experimentalists and theoreticians to carry out further work in this area.

In most cases, we have cited only the publications containing data actually used. A "floppy disk" containing the tabulated data is available from the author. Please inform the author of errors, omissions, or new data.

## 10. Acknowledgments

The author wishes to acknowledge the encouragement to complete this review by J.W. Gallagher and M. Inokuti and helpful discussions of theory and experiment with B. Brehm, W. R. Gentry, M. Inokuti, A. Russek, G. C. Schatz, and J. P. Toennies. He is particularly indebted to R. F. Stebbings for supplying data prior to publication. The support of the National Institute of Standards and Technology throughout this project is gratefully appreciated. The initial phases of this work were also supported by the Lawrence Livermore Laboratories.

## 11. References

- <sup>1</sup>E. J. Lauer, S. S. Yu, and D. M. Cox, *Phys. Rev. A* **23**, 2250 (1981).  
<sup>2</sup>M. Nahemow and N. Wainfan, *J. Appl. Phys.* **34**, 2988 (1963).  
<sup>3</sup>A. V. Phelps, *Bull. Am. Phys. Soc.* to be published; Paper NA-20, presented at the 42nd Gaseous Electronics Conference, Palo Alto, CA, October 1989 (unpublished).  
<sup>4</sup>A. C. Dexter, F. Farrel, and M. I. Lees, *J. Phys. D* **22**, 413 (1989).  
<sup>5</sup>B. M. Penetrante and E. E. Kunhardt, *J. Appl. Phys.* **59**, 3383 (1986).  
<sup>6</sup>J. R. Hiskes, *Comments At. Mol. Phys.* **19**, 59 (1987).  
<sup>7</sup>O. Fukumasa, R. Itatani, and S. Saeki, *J. Phys. D* **18**, 2433 (1985).  
<sup>8</sup>K. Frank, E. Boggasch, J. Ghristiansen, A. Goertler, W. Hartman, C. Kozlik, G. Kirkman, C. Braun, V. Dominic, M. A. Gundersen, H. Riege, and G. Mechttersheimer, *IEEE Trans. Plasma Sci.* **16**, 317 (1988).  
<sup>9</sup>B. M. Jelenković and A. V. Phelps, *Phys. Rev. A* **36**, 5310 (1987).  
<sup>10</sup>A. V. Phelps and B. M. Jelenković, *Phys. Rev. A* **38**, 2975 (1988).  
<sup>11</sup>V. T. Gylys, B. M. Jelenković, and A. V. Phelps, *J. Appl. Phys.* **65**, 3369 (1989).  
<sup>12</sup>A. E. S. Green and R. J. McNeal, *J. Geophys. Res.* **76**, 133 (1971).  
<sup>13</sup>N. V. Fedorenko, *Zh. Tekh. Fiz.* **40**, 2481 (1970); *Sov. Phys. Tech. Phys.* **15**, 1947 (1971).  
<sup>14</sup>C. L. Olson, *Phys. Rev. A* **11**, 288 (1975).  
<sup>15</sup>C. F. Barnett, J. A. Ray, E. Ricci, M. I. Wilker, E. W. McDaniel, E. W. Thomas, and H. B. Gilbody, *Atomic Data for Controlled Fusion Research* (Oak Ridge National Laboratory, Oak Ridge, TN, 1977), Vol. I of ORNL-5206.  
<sup>16</sup>H. Tawara, *Atomic Data Nucl. Data Tables* **22**, 491 (1978).  
<sup>17</sup>R. K. Janev, W. D. Langer, K. Evans, Jr., and D. E. Post, *Elementary Processes in Hydrogen-Helium Plasmas: Cross Sections and Reaction Rate Coefficients* (Springer-Verlag, Heidelberg, 1987).  
<sup>18</sup>H. Tawara, Y. Itikawa, Y. Itoh, T. Kato, H. Nishimura, S. Ohtani, H. Takagi, K. Takayanagi, and M. Yoshino, "Atomic Data Involving Hydrogens Relevant to Edge Plasmas," Institute of Plasma Physics, Nagoya University, Report No. IPPJ-AM-46, 1986 (unpublished).  
<sup>19</sup>C. F. Barnett *et al.*, "Collisions of H, H<sub>2</sub>, He, and Li Atoms and Ions with Atoms and Molecules," *Atomic Data for Fusion*, Vol. I, ORNL-6086 (1989) (in preparation).  
<sup>20</sup>E. F. van Dishoeck, E. F., and J. H. Black, *Astrophys. J. Suppl.* **62**, 109 (1986).  
<sup>21</sup>B. T. Draine and N. Katz, *Astrophys. J.* **310**, 392 (1986).  
<sup>22</sup>A. V. Phelps, in *Abstracts of Contributed Papers for International Conference on the Physics of Electronic and Atomic Collisions*, edited by J. Geddes, H. B. Gilbody, A. E. Kingston, C. J. Latimer, and H. R. J. Walters (North-Holland, Amsterdam, 1987), p. 690.  
<sup>23</sup>M. Inokuti and M. J. Berger, *Nucl. Instrum. and Methods B* **27**, 249 (1987).  
<sup>24</sup>H. W. Ellis, R. Y. Pai, E. W. McDaniel, E. A. Mason, and L. A. Vieland, *Atomic Data Nucl. Data Tables* **17**, 177 (1976).  
<sup>25</sup>C. F. Giese and W. R. Gentry, *Phys. Rev. A* **10**, 2150 (1974).  
<sup>26</sup>R. F. Stebbings, 1988 (private communication).  
<sup>27</sup>K. A. Smith, L. K. Johnson, R. S. Gao, and R. F. Stebbings, in *Abstracts of Contributed Papers for International Conference on the Physics of Electronic and Atomic Collisions*, edited by J. Geddes, H. B. Gilbody, A. E. Kingston, C. J. Latimer and H. R. J. Walters (North-Holland, Amsterdam, 1987), p. 681.  
<sup>28</sup>J. H. Newman, Y. S. Chen, K. A. Smith, and R. F. Stebbings, *J. Geophys. Res.* **91**, 8947 (1986); J. H. Newman, Y. S. Chen, K. A. Smith, and R. F. Stebbings, *J. Geophys. Res.* **94**, 7019 (1989).  
<sup>29</sup>W. H. Cramer, *J. Chem. Phys.* **35**, 836 (1961).  
<sup>30</sup>F. Linder, in *Electronic and Atomic Collisions*, edited by N. Oda and K. Takayanagi (North-Holland, Amsterdam, 1980), p. 535.  
<sup>31</sup>F. A. Gianturco and F. Tritella, *Phys. Rev. A* **16**, 542 (1977).  
<sup>32</sup>E. Gerjuoy and S. Stein, *Phys. Rev.* **97**, 1671 (1955).  
<sup>33</sup>W. R. Gentry and C. F. Giese, *Phys. Rev. A* **11**, 90 (1975).  
<sup>34</sup>R. Schinke, *Chem. Phys.* **24**, 379 (1977).  
<sup>35</sup>G. Niedner, M. Noll, J. P. Toennies, and Ch. Schlier, *J. Chem. Phys.* **87**, 2685 (1987).  
<sup>36</sup>F. A. Herrero and J. P. Doering, *Phys. Rev. A* **5**, 702 (1972).  
<sup>37</sup>M. G. Holliday, J. T. Muckerman, and L. Friedman, *J. Chem. Phys.* **54**, 1058 (1971).  
<sup>38</sup>G. Ochs and E. Teloy, *J. Chem. Phys.* **61**, 4930 (1974).  
<sup>39</sup>M. Baer, G. Niedner, and J. P. Toennies, *J. Phys. Chem.* **88**, 1461 (1988).  
<sup>40</sup>M. W. Gealy and B. Van Zyl, *Phys. Rev. A* **36**, 3091 (1987).  
<sup>41</sup>D. W. Koopman, *Phys. Rev.* **154**, 79 (1967).  
<sup>42</sup>M. E. Rudd, R. D. DuBois, L. H. Toburen, C. A. Ratcliffe, and T. V. Goffe, *Phys. Rev. A* **28**, 3244 (1983).  
<sup>43</sup>B. Van Zyl, D. Jaacks, D. Pretzer, and R. Geballe, *Phys. Rev.* **158**, 29 (1967).  
<sup>44</sup>B. Van Zyl, M. W. Gealy, and H. Neumann, *Phys. Rev.* **40**, 1664 (1989).  
<sup>45</sup>Ch. Ottinger and M. Zang, *Z. Naturforsch.* **39a**, 1296 (1984).  
<sup>46</sup>J. D. Williams, J. Geddes, and H. B. Gilbody, *J. Phys. B* **15**, 1377 (1982).  
<sup>47</sup>W. R. Hess, *Phys. Rev. A* **9**, 2036 (1974).  
<sup>48</sup>R. H. McFarland and A. H. Futch, Jr., *Phys. Rev. A* **2**, 1795 (1970).  
<sup>49</sup>E. W. Thomas, *Excitation in Heavy Particle Collisions* (Wiley, New York, 1972).  
<sup>50</sup>G. H. Dunn, R. Geballe, and D. Pretzer, *Phys. Rev.* **128**, 2200 (1962).  
<sup>51</sup>D. A. Dahlberg, D. K. Anderson, and I. E. Dayton, *Phys. Rev.* **170**, 127 (1968).  
<sup>52</sup>I. A. Sellin, *Phys. Rev.* **136**, A1245 (1964).  
<sup>53</sup>M. E. Rudd, Y.-K. Kim, D. H. Madison, and J. W. Gallagher, *Rev. Mod. Phys.* **57**, 965 (1985).  
<sup>54</sup>K. Kumar, H. R. Skullerud, and R. E. Robson, *Aust. J. Phys.* **33**, 343 (1980).  
<sup>55</sup>A. V. Phelps, B. M. Jelenković, and L. C. Pitchford, *Phys. Rev. A* **36**, 5327 (1987).  
<sup>56</sup>E. W. McDaniel, *Collision Phenomena in Ionized Gases* (Wiley, New York, 1964), pp. 19, 71-75.  
<sup>57</sup>H. S. Porter and A. E. S. Green, *J. Appl. Phys.* **46**, 5030 (1975).  
<sup>58</sup>M. E. Rudd, *Phys. Rev.* **20**, 787 (1979).  
<sup>59</sup>A. Russek, 1989 (private communication).  
<sup>60</sup>H. H. Andersen and J. F. Ziegler, *Hydrogen Stopping Power and Ranges in All Elements* (Pergamon, New York, 1977), Table 3.  
<sup>61</sup>J. F. Janni, *Atomic Data Nucl. Data Tables* **27**, 341 (1982).  
<sup>62</sup>S. K. Allison and S. D. Warshaw, *Rev. Mod. Phys.* **25**, 779 (1953).  
<sup>63</sup>J. A. Phillips, *Phys. Rev.* **90**, 532 (1953).  
<sup>64</sup>P. M. Stier and C. F. Barnett, *Phys. Rev.* **103**, 896 (1956).  
<sup>65</sup>A. V. Phelps and L. C. Pitchford, *Phys. Rev. A* **31**, 2932 (1985).  
<sup>66</sup>T. M. Miller, J. T. Moseley, D. W. Martin, and E. W. McDaniel, *Phys. Rev.* **173**, 115 (1968).  
<sup>67</sup>S. L. Lin, I. R. Gatland, and E. A. Mason, *J. Phys. B* **12**, 4179 (1979); F. Howorka, F. C. Fehsenfeld, and D. L. Albritton, *J. Phys. B* **12**, 4189 (1979).  
<sup>68</sup>G. W. McClure and K. D. Granzow, *Phys. Rev.* **125**, 3 (1962).  
<sup>69</sup>K. D. Granzow and G. W. McClure, *Phys. Rev.* **125**, 1792 (1962).  
<sup>70</sup>L. N. Pustynskii and V. P. Shumilin, *Zh. Tekh. Fiz.* **57**, 1699 (1987); *Sov. Phys. Tech. Phys.* **32**, 1016 (1987).  
<sup>71</sup>R. H. Neynaber and S. M. Trujillo, *Phys. Rev.* **167**, 63 (1968).  
<sup>72</sup>C. F. Giese and W. B. Maier, II, *J. Chem. Phys.* **39**, 739 (1963).  
<sup>73</sup>D. Shao and C. Y. Ng, *J. Chem. Phys.* **84**, 4317 (1986).  
<sup>74</sup>C. J. Latimer, R. Browning, and H. B. Gilbody, *J. Phys. B* **2**, 1055 (1969).  
<sup>75</sup>C. -L. Liao, C. -X. Liao, and C. Y. Ng, *J. Chem. Phys.* **81**, 5672 (1984).  
<sup>76</sup>A. Ding and K. Richter, *Z. Phys. A* **307**, 31 (1982).  
<sup>77</sup>B. G. Lindsay, F. B. Yousif, and C. J. Latimer, in *Abstracts of Contributed Papers for International Conference on the Physics of Electronic and Atomic Collisions*, edited by J. Geddes, H. B. Gilbody, A. E. Kingston, C. J. Latimer, and H. R. J. Walters (North-Holland, Amsterdam, 1987), p. 660.  
<sup>78</sup>P. M. Guyon, T. Baer, S. K. Cole, and T. R. Grovers, *Chem. Phys.* **119**, 145 (1988).  
<sup>79</sup>D. R. Bates and R. H. G. Ried, *Proc. Roy. Soc. A* **310**, 1 (1969).  
<sup>80</sup>C. -L. Liao and C. Y. Ng, *J. Chem. Phys.* **84**, 197 (1986).  
<sup>81</sup>C. -Y. Lee and A. E. DePristo, *J. Chem. Phys.* **80**, 1116 (1984).  
<sup>82</sup>F. A. Herrero and J. P. Doering, *Phys. Rev. Lett.* **29**, 609 (1972).  
<sup>83</sup>T. F. Moran and M. R. Flannery, *J. Chem. Phys.* **66**, 370 (1977).  
<sup>84</sup>J. H. Moore, Jr. and J. P. Doering, *Phys. Rev. Lett.* **23**, 564 (1969).  
<sup>85</sup>E. S. Zhurkin, V. A. Kaminskii, M. V. Tikhomirov, and N. N. Tunitskii, *Zh. Tekh. Fiz.* **43**, 405 (1973) [*Sov. Phys. Tech. Phys.* **18**, 259 (1973)].  
<sup>86</sup>G. W. McClure, *Phys. Rev.* **130**, 1852 (1963).  
<sup>87</sup>T. F. Moran and J. R. Roberts, *J. Chem. Phys.* **49**, 3411 (1968).  
<sup>88</sup>S. L. Anderson, F. A. Houle, D. Gerlich, and Y. T. Lee, *J. Chem. Phys.* **75**, 2153 (1981).  
<sup>89</sup>N. M. Tunitskii, E. S. Zhurkin, V. A. Kaminskii, and M. V. Tikhomirov, *Zhur. Tekh. Fiz.* **40**, 2119 (1970); [*Sov. Phys.-Tech. Phys.* **15**, 1652 (1971)].  
<sup>90</sup>C. W. Eaker and G. C. Schatz, *J. Chem. Phys.* **89**, 6713 (1988).  
<sup>91</sup>D. W. Vance and T. L. Bailey, *J. Chem. Phys.* **44**, 486 (1966).  
<sup>92</sup>J. E. Lawler, *Phys. Rev. A* **32**, 2977 (1985).  
<sup>93</sup>J. S. Townsend and F. Llewellyn Jones, *Phil. Mag.* **15**, 282 (1933).  
<sup>94</sup>G. Lange, B. Huber, and K. Wiesemann, *Z. Physik A* **281**, 21 (1977).  
<sup>95</sup>B. A. Huber, U. Schulz, and K. Wiesmann, *Phys. Lett.* **79A**, 58 (1980).

- <sup>96</sup>J. D. Williams, J. Geddes, and H. B. Gilbody, *J. Phys. D* **17**, 811 (1984).
- <sup>97</sup>K. P. Lynch and J. V. Micheal, *Int. J. Chem. Kinetics* **10**, 233 (1978).
- <sup>98</sup>S. Green and D. G. Truhlar, *Astrophys. J. (Letters)* **231**, L101 (1979).
- <sup>99</sup>K. J. McCann and M. R. Flannery, *J. Chem. Phys.* **63**, 4695 (1975).
- <sup>100</sup>H. B. Levene, D. L. Phillips, J. -C. Nieh, D. P. Gerrity, and J. J. Valentini, *Chem. Phys. Lett.* **143**, 317 (1988).
- <sup>101</sup>J. W. Ioup and A. Russek, *Phys. Rev. A* **8**, 2898 (1973).
- <sup>102</sup>R. F. Heidner, III and J. V. V. Kasper, *Chem. Phys. Lett.* **15**, 179 (1972).
- <sup>103</sup>G. C. Schatz, *Chem. Phys. Lett.* **94**, 183 (1983).
- <sup>104</sup>J. -C. Nieh and J. J. Valentini, *Phys. Rev. Lett.* **60**, 519 (1988).
- <sup>105</sup>B. M. D. D. Jansen op de Haar and G. G. Balint-Kurti, *J. Chem. Phys.* **85**, 2614 (1986).
- <sup>106</sup>J. Z. H. Zang and W. H. Miller, *Chem. Phys. Lett.* **153**, 465 (1988).
- <sup>107</sup>B. Van Zyl, M. W. Gealy, and H. Neumann, *Phys. Rev. A* **28**, 176 (1983).
- <sup>108</sup>J. H. Birely and K. J. McNeal, *Phys. Rev. A* **5**, 692 (1972).
- <sup>109</sup>B. Van Zyl, M. W. Gealy, and H. Neuman, *Phys. Rev. A* **40**, 1664 (1989).
- <sup>110</sup>B. Van Zyl, T. Q. Le, and R. C. Amme, *J. Phys. Chem.* **74**, 314 (1981); M. W. Gealy and B. van Zyl, *Phys. Rev. A* **36**, 3100 (1987).
- <sup>111</sup>C. B. Opal, W. K. Peterson, and E. C. Beaty, *J. Chem. Phys.* **55**, 4100 (1971).
- <sup>112</sup>J. Hilsenrath, C. W. Becket, W. S. Benedict, L. Fano, H. J. Hoge, J. F. Masi, R. L. Nuttall, Y. S. Touloukian, and H. W. Woolley, *Tables of Thermodynamic and Transport Properties* (Pergamon, Oxford, 1960), p. 284.
- <sup>113</sup>S. Chapman and T. G. Cowling, *The Mathematical Theory of Non-Uniform Gases* (Cambridge University, Cambridge, 1970).
- <sup>114</sup>C. A. Boitnott and R. C. Warder, Jr., *Phys. Fluids* **14**, 2312 (1971).
- <sup>115</sup>S. Green, R. Ramaswamy, and H. Rabitz, *Astrophys. J. Suppl.* **36**, 483 (1978).
- <sup>116</sup>M. M. Audibert, C. Joffrin, and J. Ducing, *Chem. Phys. Lett.* **25**, 158 (1974).
- <sup>117</sup>G. D. Billing, *Chem. Phys.* **20**, 35 (1977).
- <sup>118</sup>F. A. Gianturco and U. T. Lamanna, *Chem. Phys.* **38**, 97 (1979).
- <sup>119</sup>I. D. Williams, J. Geddes, and H. B. Gilbody, *J. Phys. B* **16**, L765 (1983).
- <sup>120</sup>B. M. Jelenković and A. V. Phelps (1986) (unpublished).
- <sup>121</sup>Z. Lj. Petrović and A. V. Phelps (1989) (unpublished).
- <sup>122</sup>R. K. Peterson and M. Eisner, *Phys. Rev. A* **8**, 1289 (1973).
- <sup>123</sup>N. Noda, *J. Phys. Soc. Japan* **43**, 1021 (1977).
- <sup>124</sup>G. W. McClure, *Phys. Rev.* **134**, A1226 (1964).
- <sup>125</sup>E. Graham, IV, D. R. James, W. C. Keever, D. L. Albritton, and E. W. McDaniel, *J. Chem. Phys.* **59**, 3477 (1973).
- <sup>126</sup>M. S. Huq, L. D. Doverspike, and R. L. Champion, *Phys. Rev. A* **27**, 2831 (1983).
- <sup>127</sup>J. S. Risley and R. Geballe, *Phys. Rev. A* **9**, 2485 (1974).
- <sup>128</sup>J. F. Williams, *Phys. Rev.* **154**, 9 (1967).
- <sup>129</sup>J. A. Stone and T. J. Morgan, *Phys. Rev. A* **31**, 3612 (1985).